# CHARACTERIZATION OF SPRAY FORMED ALUMINUM ALLOYS

A DISSERTATION

*Submitted in partial fulfillment of the requirements for the award of the degree*
*of*
MASTER OF TECHNOLOGY
in
METALLURGICAL AND MATERIALS ENGINEERING
(With Specialization in Corrosion Engineering)

By

**APARNA ZAGABATHUNI**



DEPARTMENT OF METALLURGICAL AND MATERIALS ENGINEERING
INDIAN INSTITUTE OF TECHNOLOGY ROORKEE
ROORKEE - 247 667 (INDIA)
JUNE, 2011

# CANDIDATE'S DECLARATION

I hereby declare that the work presented in this report entitled, " **CHARACTERIZATION OF SPRAY FORMED ALUMINUM ALLOYS** " in partial fulfillment of the requirements for the award of degree of **Master of Technology** in Metallurgical and Materials Engineering with specialization in Corrosion Engineering submitted to the Department of Metallurgical and Materials Engineering, Indian Institute of Technology, Roorkee, under the supervision of **Dr.DEVENDRA SINGH**, Assistant Professor, Department of Metallurgical and Materials Engineering.

I have not submitted the matter embodied in this dissertation for the award of any other degree.

Z.Aparna

Date: 30/6/11 **(Z APARNA)**

Place: IIT Roorkee

---

This is to certify that the above statement made by the candidate is correct to the best of my knowledge and belief.

**Dr. DEVENDRA SINGH**
Assistant Professor
Metallurgical and Materials Engineering
IIT-Roorkee

# ACKNOWLEDGMENT

I am deeply indebted to my guide **Dr. DEVENDRA SINGH**, Assistant Professor, Department of Metallurgical and Materials Engineering, Indian Institute of Technology roorkee, for encouraging me to undertake this dissertation as well as providing me all the necessary guidance and inspirational support throughout this dissertation work. He has displayed unique tolerance and understanding at every step of progress. It is my proud privilege to have carried out this dissertation work under his able guidance.

I am highly thankful to **Dr. P.K.GHOSH**, Professor and Head, Department of Metallurgical and Materials Engineering, Indian Institute of Technology roorkee, for providing me all necessary facilities in the department to complete this work.

I would like to thank to all my teachers here in the Department of Metallurgical and Materials Engineering who made me capable of doing all this work.

I do not have enough words to thank P.NAGESWARRAO, GOPI.M and NARASIMHA who encouraged and helped me to complete this project at the earliest.

# ABSTRACT

Processing of Aluminum alloys (Al- Graphite and Al-Si-Pb) by the conventional casting techniques is difficult due to liquid immiscibility and segregation of second phase particles during melt solidification. To overcome these problems spray forming can be used which also possesses several advantages like micro structural control together it producing a near net shape preform in less number of processing steps. In present study characterization of spray formed Al-8Graphite and Al-6Si-10Pb were studied.

Optical micrographs were taken at three different locations of the deposit viz. (a) top (b) middle and (c) bottom regions. The size of the aluminum grains was almost same at the bottom and middle regions of the deposit where as it was lower at the top region. The lead and graphite was uniformly distributed in the deposit as revealed by color dot maps. The hardness of both Al-Graphite and Al-Si-Pb are calculated and it was found that the hardness of Al-Si-Pb is more compared with Al-Graphite alloy. Preform hardness is almost constant with the increase in distance from bottom to top of the deposit. Hardness was not affected by the grain size although it decreased with the increase in porosity of the deposit.

In order to reduce the porosity, the strips were rolled to various thickness deformations in the range 20–80%. During rolling, both densification and deformation in the Al–graphite deposit take place simultaneously. In the initial stages of rolling (i.e. about 20% thickness deformation), the metal flow in the Al–graphite deposit is mainly in the thickness direction resulting in the removal of porosity by rearrangement and restacking of spray deposited particles. Beyond this, plastic deformation becomes the predominant mechanism of densification during rolling. As a result the pores are removed by a process involving pore elongation in the direction of rolling followed by fragmentation into several smaller size pores.

Friction and wear testing were investigated using a pin on disc type wear testing machine. It was observed that wear rate increases with increasing load. The coefficient of friction decreased rapidly up to 30 N and beyond this load the friction coefficient was almost constant. Feed forward back propagation neural network is used for predicting the behavior of hardness of Al-Graphite alloy. One input array is used in the construction of proposed network. It was observed that there is satisfactory agreement between the experimental and ANN results

# CONTENTS

# LIST OF FIGURES

# Chapter 1

# INTRODUCTION

Aluminum alloys are used in a wide variety of applications because of their attractive properties, such as a high strength to weight ratio, good corrosion resistance, high thermal and electrical conductivity, a low wear rate and good response to various finishing processes. Therefore, these alloys are widely used in automotive and aerospace applications. Although aluminum-silicon alloys meet many of the service requirements, such as high strength to weight ratio, excellent corrosion resistance, good bearing qualities and lower expansion characteristics, their poor resistance to seizure makes them vulnerable under poor lubricating conditions, especially during starting or warming-up of engines. In recent years, to overcome this problem, there has been an increasing trend to use solid lubricants over a broad range of applications. Suitable techniques have been also developed to disperse such solid lubricants in aluminum matrix.

Self-lubricating materials offer many improvements over the materials to which lubricant needs to be applied periodically. Among these materials, considerable work has been done on aluminum-graphite and aluminum-lead alloys. It has been shown that these alloys exhibit improvement in mechanical properties, low friction and wear, reduced temperature rise at the wearing contact surface, excellent antiseizure effects, improved machinability, low thermal expansion and high damping capacity [1]. These characteristics have made the Al-Gr and Al-Pb systems a potential candidate for automotive and general engineering applications.

Lead is soft and much cheaper and more freely available than tin. Although, it its toxic but even then a number of research efforts are being made to achieve uniform and fine distribution of Pb in immiscible systems. It is due to the fact that the applicability of Pb dispersion cannot be dispensed with in critical area. However, the low melting point of lead places an upper limit on its operational temperature range. In addition, adding elements, such as Si, Cu, and Sn to strengthen the Al matrix, the wear properties of Al-Pb alloys can be further improved [2]. Tin addition also improves the corrosion resistance of these alloys. Silicon is thought to have several benefits, including improved wear resistance, seizure resistance, strength of matrix and surface condition of the contact face [3].

Processing of Al-Pb and Al-Gr alloys by the conventional casting techniques is difficult due to immiscibility in a wide range of temperature and composition; and also large density difference of the constituent phases compared to Al alloys. Early attempts to synthesize these alloys by the conventional casting routes had limited success. A slow cooling rate associated with conventional casting processes result in rapid separation of Pb and graphite rich phases in Al matrix [4,5]. In the past, several techniques, different from conventional casting, have been employed to prevent segregation of lead and graphite during melt solidification. Techniques based on powder metallurgy [6], stir casting [7], rheocasting [8], melt spinning [9], strip casting [10], and spray forming [11] results in various distribution of lead and graphite particles in Al matrix. However, some of these techniques are often associated with either a high energy consumption or generation of coarse grain microstructures. Among these techniques spray forming possesses several advantages in effective microstructural control together with producing a near net shape preform in a less number of processing steps. Rapid cooling associated with solidification of atomized droplets and a turbulent fluid flow condition on the deposition surface minimizes the separation of Pb and graphite rich phases in Al matix [12].

Spray forming is essentially a two-step process route that involves [13]

a) Disintegration (atomization) of the molten metal by inert gas into micron-sized droplets.
b) The subsequent deposition of the mixture of solid, liquid and partially solidified droplets on a substrate surface. These droplets eventually collect as a coherent mass and the microstructure of this mass is largely dictated by the solidification conditions of the droplets during impact. Almost similar steps are used in thermal spraying process.

Above mentioned steps make spray forming a potentially attractive manufacturing route for the following reasons: [14]

1) The fast heat extraction during atomization limits large scale segregation and associated coarsening phenomena.
2) The inert conditions required for atomization and deposition minimize surface oxidation and other harmful surface reactions.

3) This process can potentially be used to produce near net shape products and thereby reducing the cost of production.

During spray atomization and subsequent deposition a detailed study of the solidification mechanisms that govern the evolution of microstructure is very complex due to the extreme differences in thermal environment both before and after impact of the droplets with the deposition surface. During spray atomization, the violent and rapid extraction of thermal energy by the atomization gas promotes the formation of highly refined grain structures. In contrast, during subsequent deposition the solidification conditions are governed by relatively slow cooling rates. The microstructure of spray-atomized and deposited materials is generally reported to exhibit spherodial or "equiaxed" grains, a feature that is consequently observed regardless of alloy composition [15]. In fact spray atomization and deposition processing exhibits the beneficial characteristics of powder metallurgy processing without the numerous processing concerns, that is, powder production, storage and handling, sintering and hot consolidation.

Various shapes like disc, billet, tube and ring can be produced by this process. The disintegration or atomized droplets during the process follow a particular distribution and therefore some special arrangements are required to produce aforementioned shapes of desired dimensions. The produced part also has some porosity [16] which can be shrinkage porosity, gas porosity etc.

In the present work characterization of spray formed aluminum-graphite and aluminum-silicon-lead were studied. Hardness, wear rate, coefficient of friction, optical microstructure, SEM, EDAX analysis, Effect of rolling, Artificial neural network have been carried out for the purpose.

# Chapter 2

# LITERATURE REVIEW

Due to single-step processing cycle, spray-formed aluminum alloys can be produced at substantially lower cost than powder metallurgy products, approaching cost levels of direct chill (DC) cast alloys at high production volumes. The comparison between the steps involved in three types of processing routes to produce metal part is given in Fig 2.1. It shows that number of processing steps is reduced in spray forming to form end product.

## 2.1 BEARINGS MATERIALS

Bearing material [17] should have the following characteristics:

a) Embeddability, to allow hard particles to embed in the bearing material.
b) Compatibility, to avoid damaging or roughening the counter face.
c) Conformability, to accommodate alight misalignment in the bearing system.
d) High strength, to support applied loads.
e) Fatigue resistance and corrosion resistance for a longer service life.

To compromise and satisfy these conflicting demands, most bearing material contain two phases. One is soft and ductile phase, which provides good embeddability and conformability; the other is a hard and strong phase which has strength and fatigue resistance. Traditionally, soft metal elements such as Pb, Sn, In and Bi are incorporated in harder metal elements such as Cu and Al to produce alloys for bearing applications. Al based alloys have the advantage of high strength to weight ratio, and therefore they are widely used in the automotive industry. Immiscible alloys, such as Al-Gr, Al-Pb, Al-In and Al-Bi alloys, cannot be cast using conventional casting methods due to large density difference between two phases in their liquid state. Several methods have been proposed to produce immiscible Al-graphite, Al-lead alloys, such as stir casting, rheocasting, rapid solidification and spray forming. Techniques based on ultrasonic vibration of melt, powder metallurgy, stir casting, space metallurgy, rheocasting, melt spinning, strip casting and spray forming, result in a uniform distribution of graphite and lead particles in Al matrix. However, some of these techniques are often associated with either a high energy consumption or generation of coarse grain microstrucutres.

Among these techniques, spray forming possesses several advantages in effective microstructural control together with producing a near net shape perform in a lesser number of processing steps. In this process, the melt is superheated to a temperature above the liquid immiscibility region of the melt prior to its atomization.

Rapid cooling associated with solidification of atomized droplets and a turbulent fluid flow condition on the deposition surface minimizes the separation of the graphite and Pb rich phases in Al matrix. However, a high melt temperature results in rapid coarsening of graphite and lead particles in this process.

Rohatgi [18] states that Al-graphite composite is used in bearing due to its special features such as cheaper, lighter, self lubricating, conserves copper, lead, tin, zinc etc. he also states that Al-graphite cast metal composition can also be used in automobile pistions due to its reduction in wear and antiseizing property. He states that compositions produced from powder metallurgy route have certain advantages over liquid metallurgy:

1. At low temperatures, composite formed in powder metallurgy route have better mechanical properties than liquid metallurgy one.
2. Several composites such as Al-graphite cannot be formed from liquid metallurgy. Higher graphite content cannot be introduced through liquid metallurgy route due to wide differences in density and non wetting characteristics of graphite with aluminum.

S.Mohan [19] compare Al-Pb and Al-Sn alloys. Besides being cheaper, lead ensures a better interfacial film of lubricant than tin. Due to mutual immiscibility and large difference in density the production Al-Pb alloys by conventional casting techniques poses problem of segregation. So he uses following dispersion techniques.

1. Liquid-liquid dispersion at elevated temperature by stircasting.
2. Liquid-solid dispersion by rheocasting.
3. Inserting lead alloy wires in to the liquid Al and quenching it.

## 2.2 SPRAY FORMING

Spray forming, also called spray casting or spray deposition, is the inert gas atomization of a liquid metal stream into variously sized droplets which are then propelled away from the region of atomization by the fast flowing, atomizing gas. The droplet trajectories are interrupted by a substrate which collects and solidifies the droplets into a coherent, near fully dense preform. This method has many advantages over conventional techniques like casting, powder metallurgy etc. in one particular method of spray forming, a stream of molten metal falling freely under gravity is atomized by a system of high pressure jets to form the required plume or spray of droplets which, when they impinge on the suitably shaped receptor under appropriate conditions build up to form a solid artifact for subsequent hot compaction as required. Hitherto, it has been possible to produce sheets or plates of relatively thick section by such methods: however the correct conditions for the continuous production of near to final thickness strip have not been established. Spray forming techniques can be used to produce a wide variety of metallic strips of different compositions [13].

### 2.2.1 ADVANTAGES

One of the major advantages of spray forming is the ability to develop new alloys or products. These include new alloy compositions as a result of rapid solidification; MMCs formed by injecting particulate in to the metal spray; in-situ reactive alloys created by creating a reaction between a constituent of the alloy to be sprayed and a constituent of either the atomizing gas or an injected particulate or by mixing sprays of different alloy compositions.

**Fine scale microstructure**

The characteristic microstructure of as-spray formed preforms typically consists of refined (10-100 pm) equiaxed grains, usually with low levels of internal solute partitioning and refinement of intermetallic dispersoids, secondary precipitates and eutectic phases.

**Near net shape**

The ability to spray form large near net shape extrusion/forging preform tubes, rolls and strips with fine scale microstructures in large cross-sections directly from the melt offers potential economic benefits in comparison with both ingot metallurgy (IM) and powder metallurgy (PM) routes. Spray forming reduces the multiple PM operations of powder production, sieving, canning, degassing and consolidation to a single operation, while retaining a PM type microstructure in near net shapes. Problems associated with powder handling, such as

combustion or contamination by surface oxide formation, which inhibits particle bonding during consolidation and impairs mechanical properties, are also avoided.

**Improved workability**

The spray forming technology provides improved hot workability because of improved homogenization of alloy chemistry and a reduction of the grain size inherent in gas-atomization processing. The spray formed product is also extremely clean, compared with conventional remelt stock, and has minimal segregation because of rapid solidification. The microstructure is typically homogeneous.

**Less number of steps**

As compared to conventional casting techniques and powder metallurgy spray forming process has less number of steps. In spray forming we directly get a preform after atomization and deposition.

**Flexibility**

Spray forming is able to manufacture a wide range of materials, some of which are difficult to produce by other methods, including alloys of Al, Pb, Cu, Mg, Ni, Ti, Co and steels.

### 2.2.2 DISADVANTAGES

As-spray formed preforms always contain some porosity, and are usually consolidated to full density by extrusion, hot/cold rolling. Additional subsequent heat treatment and/or forging operations are used to optimise microstructural and mechanical characteristics, during which there is usually some microstructural coarsening. The efficiency of feedstock conversion to final product (yield) by spray forming is usually significantly below 100%. Material losses arise from:

a) Overspray of droplets which do not impact on the preform top surface;
b) Bounce off of impacting droplets or powder from the preform surface;
c) Scalping or machining losses from out of specification preforms and the removal of preform bases and crowns; and
d) Preform rejection because of insufficient metallurgical quality.

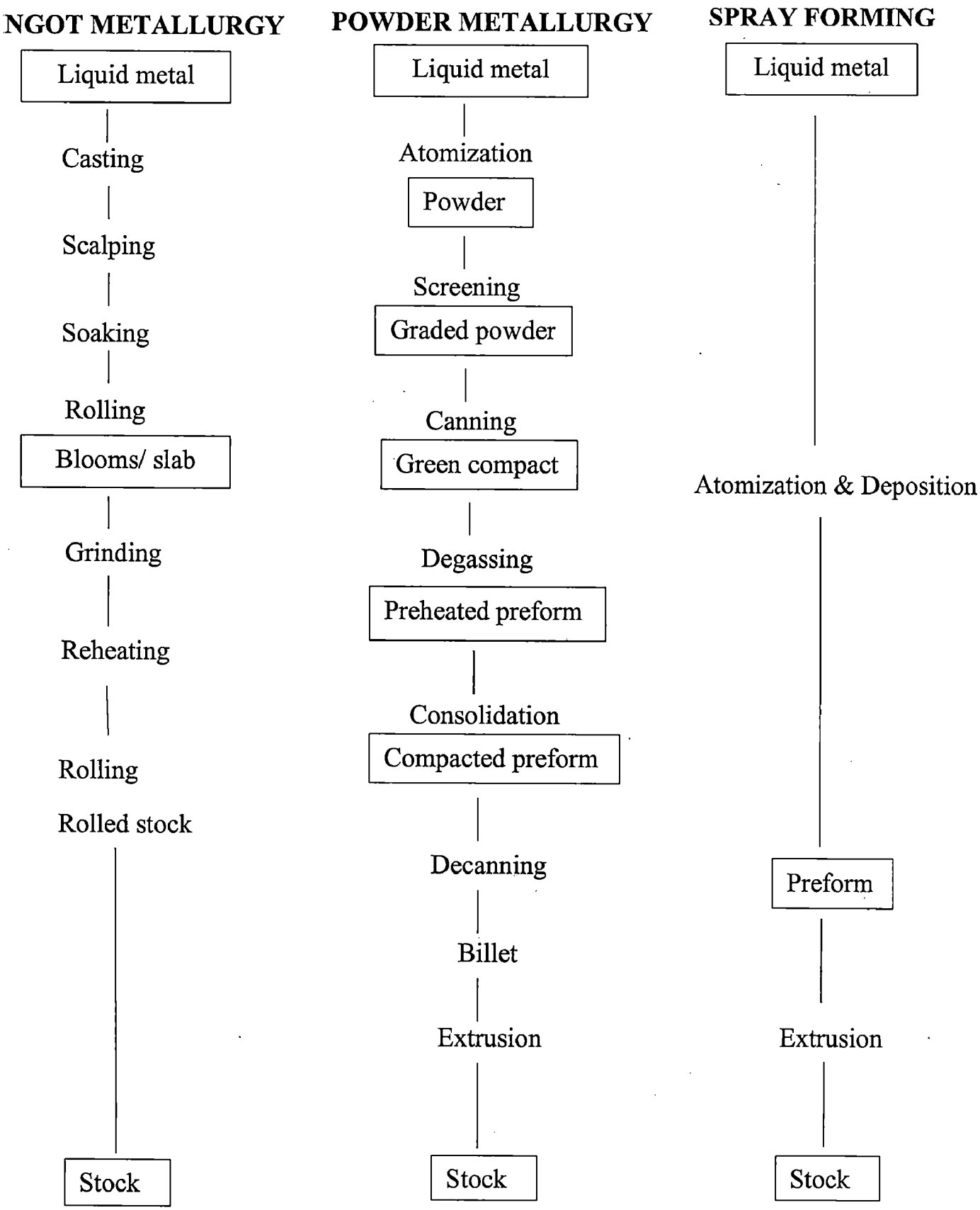


**Figure 2.1** Comparison of processing steps involved in three types of processing routes.

## 2.3 HISTORY OF SPRAY FORMING

Spray forming being an emerging technology consists of a very few processing steps than the other emerging technologies like powder metallurgy. This process can be applied to a variety of ferrous and non-ferrous alloys and composites.

The concept of spray forming has come into existence in early 1970's. prof. Singer pioneered the spray forming process at Swansea university, Wales, in the early 1970s as the spray rolling process. His work was confined to Al alloys. Later on spray forming was further developed and subsequently licensed by Osprey metals, neath, Wales, in early 1980s and consequently spray forming is often referred to as the "Osprey process". Further in the late 1980s liquid dynamic compaction (LDC) process which is similar to spray forming was developed by Lavernia and Grant. It is worthwhile to point out here that LDC, Osprey process, and spray forming is the generic names of similar or related processes. The melt in LDC was atomized at a high-gas pressure to generate the maximum yield of small size droplets in the spray. The cooling rate of large fraction of droplets was well within the rapid solidification regime.

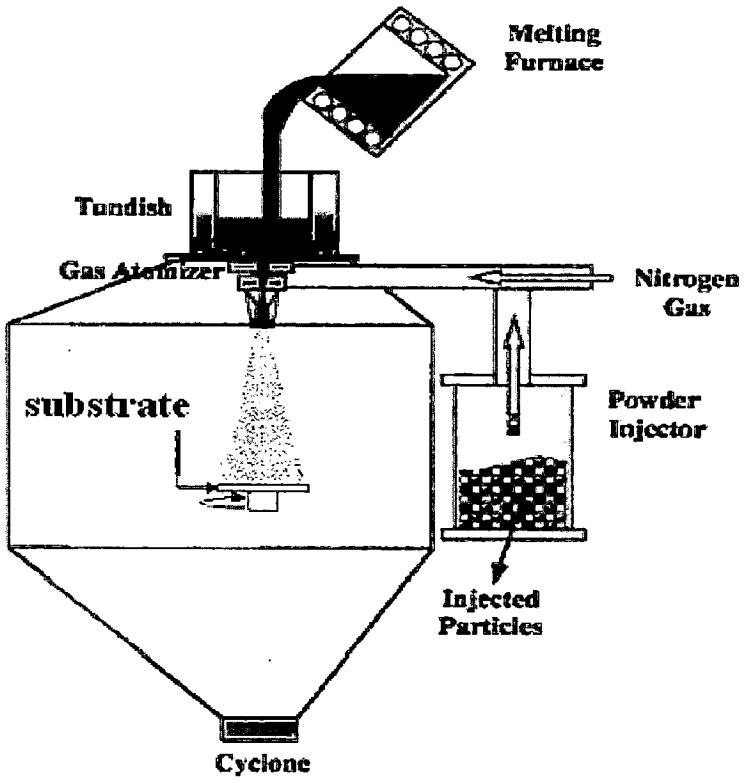


**Figure 2.2** Schematic of spray forming process for the manufacturing of billets, tubes and strips

Spray forming offers certain advantages over both conventional ingot metallurgy and more specialist techniques such as powder metallurgy. Firstly, it is flexible process and can be used to manufacture a wide range of materials, some of which are difficult to produce by other methods, e.g. Al-5wt%Li alloys or Al-SiC, Al-Al2O3 metal matrix composites (MMCs). The atomization of the melt stream into droplets of 10-500mm diameter, some of which, depending on diameter, cool quickly to the solid and semi solid state provide a large number of nucleants for the residual liquid fraction of the spray formed material on the billet top surface. The combination of rapid cooling in the spray and the generation of large population of solid nucleants in the impacting spray leads to a fine equiaxed microstructure, typically in the range 10-100mm, with low levels and short length scales of internal solute partitioning. These microstructural aspects offer advantages in material strength because of fine grain size, refined distribution of dispersoid and secondary particulate phases, as well as tolerance to impurity 'tramp' elements. This fine structure in the 'as-sprayed' condition means homogenizing heat treatments can often be avoided. Because of the complex solidification path (i.e. the rapid transition from superheated melt to solid, liquid or semi-solid droplet to temperature equilibration at semi-solid billet top and final slow cooling to fully solid) of the spray formed material, extended solubility of allying elements and the formation of metastable and quasi-crystalline phases has also been reported.

One of the major attractions of spray forming is the potential economic benefit to be gained from reducing the number of processing steps between melt and finished product. Spray forming can be used to produce stip, tube, ring, clad bar/ roll and cylindrical extrusion fedd stock products, in each case with a relatively fine-scale microstructure even in large cross-sections. The benefits of GASF over powder metallurgy accrue from the reduced number of process steps where powder sieving, pressing, de-gassing and handling steps and their attendant safety and contamination issues may be removed.

## 2.4 BASIC STEPS INVOLVED IN SPRAY FORMING

Spray forming consists of the sequential steps of:

1) Atomization of liquid materials to create a droplet spray
2) Control of the resulting droplet spray in the gas flow field to achieve a desired droplet mass and enthalpy distribution prior to deposition; and
3) The deposition of droplets at a surface to build up a pre-defined performs.

Fig.2.2 shows the spray forming of a preform, indicating the approximate physical regions for the melt atomization, droplet flight and droplet deposition steps. Spray forming is an inherent multi-physics process consisting of multi-length (microns to meters) and multi-time scale (microseconds to minutes) transport phenomena

The basic physics involved are;

1. The fragmentation of a continuous liquid stream in to discrete droplets;
2. Multi-phase flow of the gas-droplet spray cone and non-linear heat transfer;
3. Droplet deposition, splashing and re-deposition; and
4. Perform solidification and microstructure evolution.

The multi-scale, dynamic and nonlinear nature of the inter-related physics of the spray formed process present a significant challenge for the development of meaningful numerical models of the process. The atomization process plays an essential role for processes like spray forming as it primarily influences the shape of the sprayed deposit as well as its material properties. In the atomization stage, the mass flux distribution and enthalpy density distribution in the spray are determined, resulting from the different sizes of droplets and particles and their thermal histories during flight in the spray cone from the atomization zone to the impingement onto the deposit surface. In comparison to conventional liquid atomization processes (e.g. atomization of water based liquids), atomization of metal melts in spray forming is more complicated due to the high temperature of the hot melt and the high temperature gradients between the melt and the cold atomization gas. In addition the material properties of both phases change over a wide range due to temperature variations. The purpose of the investigation is to understand and describe the main driving mechanisms of the atomization process as a base for modeling of the overall disintegration process and to derive possibilities of direct influencing the resulting spray properties from the atomization process.

Spray forming or spray deposition is the inert gas atomization of the liquid metal stream which contains variously sized droplets, which are propelled away from the region of atomization by the fast flowing atomization gas. The droplet motion is interrupted by a substrate which collects and solidifies the droplet into a coherent nearly fully dense preform as shown in Fig 2.2. The droplet formed during atomization are cooled both by convention as well as radiation mode of heat transfer during the flight. Thus these droplets experience high cooling rates. High cooling rate of droplets are also due to increased surface to volume ratio. Since

different cooling rates are encountered for various size droplets, they posses unlike thermal states away from the atomization zone. The large droplets experience slower cooling rate than that of the smaller one which completely solidify due to high cooling rates. Intermediate sixe droplets remain in a musty state. These droplets when impinge on to the substrate, get fragmented and this leads to grain multiplication. Entire spray forms a semi-solid/liquid pool on the top surface of the preform. The large mass fraction is confined to the central region of the preform. Thus the shape of perform depends upon the flat mass flux distribution of droplets in the spray.

### 2.4.1 PROCESS PARAMETERS IN SPRAY FORMING PROCESS:

The various process parameters in a spray forming process are as follow:

1. Melt to gas ratio
2. Flow rate of molten metal
3. Atomization gas pressure
4. Distance between the nozzle and the substrate and the orientation of the substrate.

These parameters play a vital role in refining the microstructure of the preform and thereby enhance the mechanical and wear properties. These independent process parameters can be directly controlled during the process and affect a number of dependent process parameters like the state of spray at deposition and the state of the deposition surface. Therefore, these process parameters should be controlled to produce the optimum mixture of liquid and solid droplets that are essential for producing a quality perform

At the bottom of the preform, microstructure is much refined due to very high cooling effect produced by substrate through conduction. But as the thickness increases, cooling rate decreases and therefore coarse grains are obtained.

On the top of the preform, radial temperature gradient is approximately zero and heat transfer takes place through the preform is very low in radial direction. Therefore, the most of heat transfer takes place by convection through the high velocity gas flowing on the top of the perform surface. Hence, a uniform microstructure is developed throughout the preform after the chill zone near the substrate. If metal/gas mass flow ratio is higher, then larger size droplets will form in the spray and thus lead to coarse microstructure. An increase in initial gas velocity results in reduction of flight time and an increment in mean heat transfer coefficient and thus cooling rate increases where as reduction of droplets size leads to increase solid fraction. Solid fraction during flight or in spray can be calculated from the models incorporating different

process variables. The combination of droplet and perform solid fractions determine the way in which droplets either bounces off the preform or incorporated. It is depicted that a high liquid content at the surface of perform results in excessive whipping and splashing of liquid leading to the loss of material. In other case when both, droplets and perform are in solid state, total bounce-off of the particles occurs. In some cases when spray consists of fully liquid droplets and perform remains solid, a layered structure is formed. Best sticking is obtained when deposit remains in mushy state and spray consists of mushy or liquid droplets. Large liquid fraction in the spray with high heat content leads to a coarse microstructure.

Therefore, it can be concluded that optimum control of the process parameters is necessary to obtain a required microstructure. There are several process parameters which effect perform integrity which have been identified in the spray atomization and deposition processing as enumerated below:

1. Melt superheat (50-250°C).
2. Melt flow rate.
3. Gas pressure.
4. Nozzle to substrate distance.
5. Substrate motion, which includes substrate rotation speed, withdrawal rate, tilt angle.

In addition to these there are several pre-set (or design) parameters which can be selected prior to, but not during, the operation of process. These are given below

1) Melt flow tube diameter.
2) The type of atomizing gas.
3) Substrate material.
4) The gas atomizer design.

## 2.5 PERFORM CHARACTERIZATION OF AL-SI-PB AND AL-GRAPHITE ALLOYS

There is not much literature available on Al-Si-Pb spray formed alloys and their characteristics. The process parameters include the alloy composition, gas pressure used for spray forming, melt temperature of the alloy and deposition distance i.e. distance between atomizer and substrate. The alloy characterization parameters include the microstructure of the alloy, its porosity, applied wear load, sliding speed during wear, wear rate, coefficient of friction, spray formed or cast alloy, its hardness, stress and percent elongation to fracture.

An et al. [6] have investigated the wear behavior of as cast and hot extruded Al-Si-Pb alloys under dry conditions using a pin on disc type wear testing machine. The results shown almost constant wear rate at intermediate load levels. The wear rate in Al-Si-Pb alloys was found to decrease with increasing lead content. Better resistance to seizure for Al-Si-Pb alloys with more than 15wt% lead was observed due to a film of lubricant covering almost the entire worn surface. This film was a mixture of different constituents containing Al, Fe, Si, O and Pb. Pathak et al. studied the wear characteristics of a series of leaded aluminum bearing cast alloys under dry sliding conditions under a room atmosphere using a pin on disc type wear testing machine. The wear volume was measured as a function of the alloy composition, sliding distance, normal load and sliding velocity. Optical and scanning electron microscopic examinations of the test specimen wear track and wear debris were carried out to aid in the elucidation of the wear mechanisms. It was observed generally that the wear rate decreased with increasing lead content and hardness of aluminum based alloys. They also have studied the antiseizure and antifriction characteristics of a number of Al-Si-Pb as cast alloys with silicon contents in the range 2-20wt% and lead contents in the range 0-10 wt% under different lubricating conditions using a bearing test machine. The addition of lead to aluminum –silicon alloys was generally found to reduce interfacial friction and improve their ability to resist seizure. A lower friction coefficient and a higher seizure load were obtained for Al-Si-Pb alloys bearing in semi-dry sliding conditions compared with those were observed for dry conditions.

Sharma and Rajan [20] investigated the coefficient of friction characteristics of cast aluminum-silicon alloy with varying lead content from 4 to 16 wt% under lubricated, semi-dry and dry conditions. The average value of coefficient of friction in the oil-lubricated test was lower as compared with semi-dry and dry tests. In general the influence of morphology of microstructure, lead distribution and addition of lead was found helpful in reducing interface friction. They also studied wear of Al-12Si and Al-12Si-1Cu-1.5Mg alloys along with varying amounts of lead (from 4 to 16 wt%). Wear experiments were conducted on a pin on disc machine. The worn out test pin surface topography, sub-surface damage and debris were studied by scanning electron microscope (SEM). The worn out test pin surfaces for all the alloys showed a multitude of distinct topographical features in the SEM images. It was found that a number of wear processes, such as delamination, adhesion and abrasion, take part in removal of metal as

debris, and no single wear process is responsible for metal removal from sliding surface. The presence of lead in base alloys was found to reduce wear and friction.

Fang and Fan [8] successfully produced immiscible Al-Si-Pb alloys using the rheo-diecasting process (RDC). The microstructure of RDC Al-Si-Pb alloys was characterized by spherical and fine Pb particles dispersed uniformly in the Al-Si alloy matrix. The size of the α-Al primary phase was approximately 50μm and the average size of the Pb particles increased with the increase in Pb concentration. The Pb particle size increased from 2.6 μm in Al-7Si-17.2Pb alloy. It was also found that both the ultimate tensile strength and elongation of Al-Si-Pb alloys decreased with increasing Pb content.

Rudrakshi et al. [11] spray formed Al-Si-Cu-Pb at a gas pressure of 1.0MPa and the nozzle to substrate distance was varied from 0.35 to 0.55m. the microstructure and the wear characteristics of the spray deposits were investigated. The results invariably exhibited and equiaxed grain morphology of the primary α-phase with variation in grain size from 10 to 25 μm in addition to a uniform dispersion of ultra-fine particles of lead and globular silicon particles in Al-matrix. The size of Si particles varied from 0.5 to 5 μm and that of Pb particles from 0.1 to 25μm with variation in deposition distance. The microstructural variation was also observed in different regions of the deposit. The atomized powder particles revealed two different types of microstructures, the one showing a cellular-dendritic morphology of the primary α-phase where as the other exhibited fine spherical Al-particles dispersed in the matrix of Pb rich phase. The wear rate and the coefficient of friction of Al-Si-Cu-Pb alloy were observed to be lower than of Al-Si alloy at loads varying from 10 to 90 N at a sliding velocity of 1.0 m/s.

Rudrakshi et al. [12] also have studied the wear behavior of same alloys in different environmental conditions. The wear tests were carried out in air atmosphere and vacuum, using a pin on disc type wear testing equipment. The wear behavior in air atmosphere clearly indicated the influence of surface oxidation on the mating surfaces. This related in the formation of irregular shaped oxide particles having bright contrast in SEM investigation of worn surfaces and debris particles. The nature of variation in wear with sliding distance, both in air atmosphere and vacuum, remained similar showing two distinct wear regmies, viz., running in wear and steady state wear. A relatively lower running in period and a large reduction in the frictional force were observed in vacuum as compared to that obtained in air under same conditions of sliding speed and applied pressure. The wear rate varied from (0.25 to 0.61)x10-12 $m^3/m$ for a range of applied

pressure of 0.2-1.8 MPa and at a constant sliding speed of 1.0m/s in vacuum, whereas, the wear rates observed in air atmosphere for the same sliding conditions range between (0.75 and 3.87)x10-12 $m^3/m$. the coefficient of friction in air atmosphere varied fro low pressures and remained almost constant at 0.25 in high pressure regime, whereas in vacuum it decreased linearly and finally attained a constant value of 0.1. The wear rate increased with sliding speed in vacuum, on the other hand, in air atmosphere the wear rate decreased with increasing sliding speed, reaching a minimum at a critical sliding speed and then increasing with further increase in sliding speed. The coefficient of friction remained almost constant for different sliding speeds for both air and vacuum. However, under vacuum, the value of coefficient of friction was lower than that in air, through the range of sliding speed.

Yu. et al. [21] produced Al-11.5Si-15Pband Al-18Si-10Pb alloys by liquid phase co-spray forming. Some deposit was extruded and then microstructure and tensile properties were studied. Torabian et al. [22]studied wear characteristics of Al-Si-Pb alloys with silicon content from 2 to 20 wt% and lead from 2 to 10 wt% using a pin on disc type wear testing machine at room temperature. The affects of applied load, sliding velocity and alloy composition on wear rate of Al-Si-Pb alloys were investigated. It was found that wear rate strongly depend on alloy composition, applied load and sliding speed. Wear rate decreased and load bearing capacity of the alloy increased with the increased in lead content. Wear rate of Al-Si-Pb alloys initially decreased and then increased with the increase in sliding speed.

M. Saravanan, R.M. Pillai, [23] successfully produced immiscible Al-5vol% graphite alloy using equal channel angular pressing (ECAP). ECAP of Al–5 vol.% Grp composite has been successfully carried out up to four passes at room temperature. A significant grain refinement, down to the submicron level of 300 nm, is achieved in Al–GrP composite. Hardness enhancement of more than two fold was observed with only a marginal difference along the perpendicular and parallel directions of pressing. Further, the strength of the composites is increased more than two folds by ECAP. It was found that ECAP results in more rapid and significant grain refinement and strengthening in Al–GrP composite at room temperature.

F. Akhlaghi, S.A. Pelaseyyed, [4] produced Al-graphite composite by in-situ powder metallurgy. The microstructure and wear characteristics of the composite were investigated. A fine and relatively uniform grain size in the range of 10–20μm was observed. The average size of the eutectic silicon particles within the powder particles, as measured by an image analyzer, was

3μm. The wear test was carried out using a pin on disc type wear testing equipment. It was observed that, the effect of the graphite addition in reducing the wear and friction of the composites is due to formation of a thin lubricating graphite rich film on the tribosurface and secondly, the adverse effects of the graphite addition in formation of porosity and cracks as well as the deterioration of mechanical properties resulting in enhanced delamination.

I. Estrada-Guel, C. Carreno-Gallardo, [24] produed Al7075 alloy from elemental powders and reinforced with metallized graphite nanoparticles (GNP) by mechanical alloying (MA). It was observed that original particles were semi-spherical, typical of gas-atomized powders, and had small satellite particles attached to large particles. After 2.5 h of milling, the particles were severely deformed plastically by MA and exhibited a shape changes from nearly spherical to flake-like particles. Density variation versus milling time indicates severe plastic deformation of the aluminum powder during milling which form flake-like particles with low density during the early stages of processing; when the hardening particles were added, they accelerated the milling process of the aluminum matrix, reached a stable state condition, and; consequently, the density rate increases considerably. Tensile test and hardness measurements for the prepared composites show a significant increase (40%) in maximum tensile strength and in hardness (20%) as compared to the blanks (as-mixed and extruded sample).

## 2.6 ARTIFICIAL NEURAL NETWORK

Artificial neural networks are considered as artificial intelligence modeling techniques. They have a highly interconnected structure similar to brain cells of human neural networks and consist of the large number of simple processing elements called neurons, which are arranged in different layers in the network; an input layer, an output layer and one or more hidden layers. One of the well-known advantages of ANN is that the ANN has the ability to learn from the sample set, which is called training set, in a supervised or unsupervised learning process [25]. Once the architecture of network is defined, then through learning process, weights are calculated so as to present the desired output. Several different architecture and topologies have been proposed for ANN. They differ in terms of architecture, learning process and training strategies.

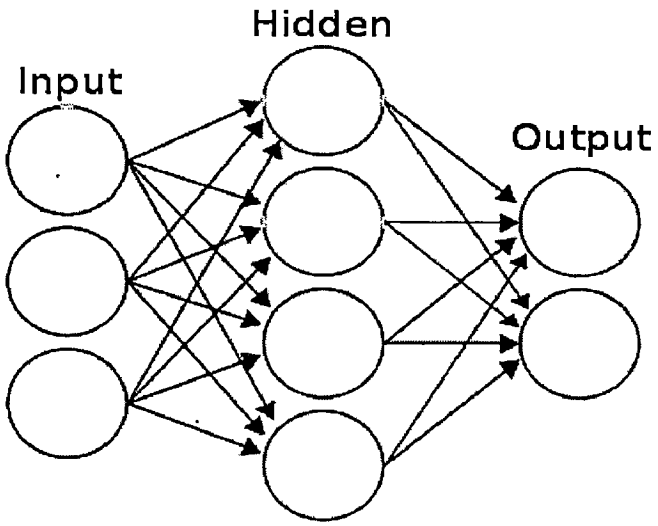


**Figure 2.3** Neural network

### 2.6.1 LEARNING PARADIGMS

There are three major learning paradigms, each corresponding to a particular abstract learning task. These are supervised learning, unsupervised learning and reinforcement learning.

### 2.6.2 SUPERVISED LEARNING

In supervised learning, we are given a set of example pairs $(x, y), x \in X, y \in Y$ and the aim is to find a function $f: X \to Y$ in the allowed class of functions that matches the examples. In other words, we wish to infer the mapping implied by the data; the cost function is related to the mismatch between our mapping and the data and it implicitly contains prior knowledge about the problem domain. A commonly used cost is the mean-squared error, which tries to minimize the average squared error between the network's output, *f(x),* and the target value y over all the example pairs. The supervised learning paradigm is also applicable to sequential data (e.g., for speech and gesture recognition). This can be thought of as learning with a "teacher," in the form of a function that provides continuous feedback on the quality of solutions obtained thus far.

### 2.6.3 UNSUPERVISED LEARNING

In unsupervised learning, some data $x$ is given and the cost function to be minimized, that can be any function of the data $x$ and the network's output, $f$. The cost function is dependent on the task (what we are trying to model) and our prior assumptions (the implicit properties of

our model, its parameters and the observed variables .Tasks that fall within the paradigm of unsupervised learning are in general estimation problems; the applications include clustering, the estimation of statistical distributions, compression and filtering.

### 2.6.4 REINFORCEMENT LEARNING

In reinforcement learning, data $x$ are usually not given, but generated by an agent's interactions with the environment. At each point in time $t$, the agent performs an action $y_t$ and the environment generates an observation $x_t$ and an instantaneous cost $c_t$, according to some (usually unknown) dynamics. The aim is to discover a *policy* for selecting actions that minimizes some measure of a long-term cost; i.e., the expected cumulative cost. The environment's dynamics and the long-term cost for each policy are usually unknown, but can be estimated. Tasks that fall within the paradigm of reinforcement learning are control problems, games and other sequential decision making tasks.

### 2.6.5 LEARNING ALGORITHMS

Training a neural network model essentially means selecting one model from the set of allowed models (or, in a Bayesian framework, determining a distribution over the set of allowed models) that minimizes the cost criterion [26]. There are numerous algorithms available for training neural network models; most of them can be viewed as a straightforward application of optimization theory and statistical estimation.

Most of the algorithms used in training artificial neural networks employ some form of gradient descent. This is done by simply taking the derivative of the cost function with respect to the network parameters and then changing those parameters in a gradient-related direction. Evolutionary methods, simulated annealing, expectation-maximization and non-parametric methods are some commonly used methods for training neural networks.

Temporal perceptual learning relies on finding temporal relationships in sensory signal streams. In an environment, statistically salient temporal correlations can be found by monitoring the arrival times of sensory signals. This is done by the perceptual network.

Perhaps the greatest advantage of ANNs is their ability to be used as an arbitrary function approximation mechanism that 'learns' from observed data. However, using them is not so straightforward and a relatively good understanding of the underlying theory is essential [27].

- Choice of model: This will depend on the data representation and the application. Overly complex models tend to lead to problems with learning.
- Learning algorithm: There is numerous trades-offs between learning algorithms. Almost any algorithm will work well with the correct hyper parameters for training on a particular fixed data set. However selecting and tuning an algorithm for training on unseen data requires a significant amount of experimentation.
- Robustness: If the model, cost function and learning algorithm are selected appropriately the resulting ANN can be extremely robust.

With the correct implementation, ANNs can be used naturally in online learning and large data set applications. Their simple implementation and the existence of mostly local dependencies exhibited in the structure allows for fast, parallel implementations in hardware.

# Chapter 3

# EXPERIMENTAL PROCEDURE

In this chapter the experimental details used for the study has been summarized.

## 3.1 Spray forming procedure

Desired amount of aluminum was melted in a crucible, under nitrogen atmosphere, to a temperature much higher than melting temperature of aluminum so as to provide superheat. The heating was carried for about 1 hour. A stopper rod runs through the centre of the charge and locates in the top of a delivery nozzle at the base of the crucible. The thermocouple in the centre of the stopper rod allows continuous measurement of the charge temperature. When a pre-determined temperature is reached (1100 K for Al-Graphite and 600K for Al-Si-Pb), the high pressure nitrogen gas flow is started through the atomizer assembly, the stopper rod is raised and the molten metal flows through the delivery nozzle. The pressure of nitrogen was made 10 bar by compressor. Graphite is injected in to the chamber by using ceramic injectors. The molten metal stream exits into the deposition chamber and is atomized into variously sized droplets by the impinging energetic gas stream. To compensate for the decreasing melt hydrostatic pressure and corresponding decrease in melt mass flow rate as spraying proceeds, a gradual increase in a nitrogen gas melt overpressure is sometimes used. Atomized droplets are propelled down the chamber to be collected at the substrate which is usually moved, either by rotation or lateral withdrawal, through all regions of the spray cone to average variations in spray density over the surface of the preform. Deposition is complete when the metal flow is exhausted. Overspray is continuously removed from the chamber to a cyclone [28]. The deposit collected on the substrate had a variation in thickness along the longitudinal direction of the substrate. The thickness was maximum at the center and minimum at the edges of the deposit along the longitudinal direction. However, the variation in thickness of the deposit along the transverse direction of the substrate was not significant.

## 3.2 Perform characterization

Preform produced by spray forming process is characterized by the properties reported below.

The shape of the as-received spray formed preform is shown in Figure 3.1. Disc was characterized and the following results were obtained.

**Figure 3.1** Shape of the spray deposit produced on substrate.

Samples for microstructural and hardness investigation were cut from central region of perform as shown in Figure 3.2.

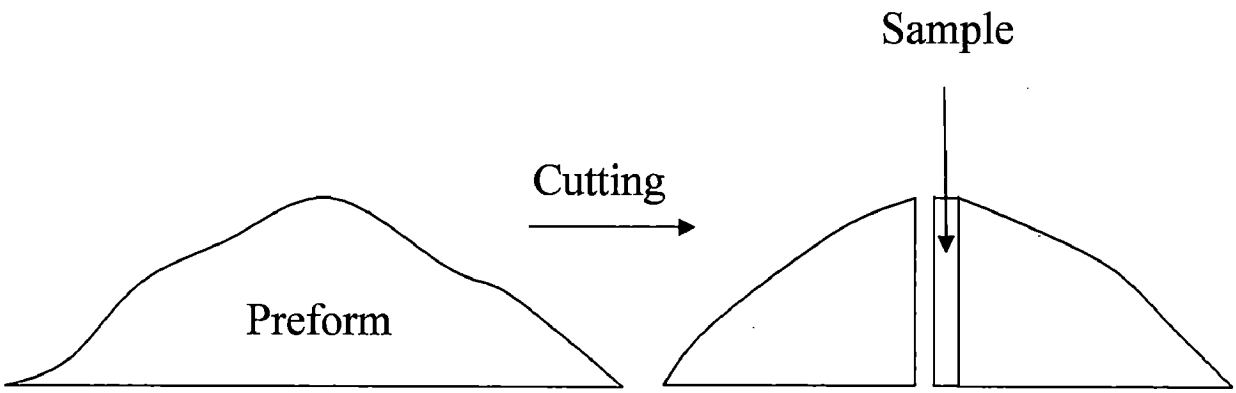


**Figure 3.2** Cutting of sample in strip form from perform for micro-structural and hardness study.

### 3.2.1 MICROSTRUCTURE

Samples from the central regions of the preform (as shown in fig) were cut down for its micro-structural study. These samples were polished using standard metallographic technique of polishing with an emery paper of 1/0, 2/0, 3/0 and 4/0 specification and then followed by wheel cloth polishing using an emulsion of aluminum powder particles suspended in water. After final polishing the samples were cleaned with acetone and etched with Polton's reagent for three minutes. Microstructure was examined with LEICA DMI 5000 M Optical microscope under polarized light

### 3.2.2 EDAX ANALYSIS

Phases present in spray formed aluminum alloy perform were examined by EDAX analysis technique. Samples were scanned at various locations under SEM and the critical area of interest was studied with an aim to identify the morphology of the cross-section of the preform.

### 3.2.3 HARDNESS

Samples for hardness investigation were cut from central and peripheral regions of preform as shown in the fig. before commencement of test, samples were ground and polished using standard metallographic techniques. A Brinell-cum-Vicker's hardness tester was used to measure the Vicker hardness at 5 Kg load. Indentations were taken at different points of central and peripheral regions of each sample.

### 3.2.4 WEAR TESTING

The spray formed perform were machined into cylindrical pins of dimensions 8mm diameter x 30 mm length. Specimens were thoroughly degreased by acetone and dried before the commencement of each wear test.

Friction and wear testing of spray formed alloys were investigated using a pin on disc type wear testing machine. It consisted of a hardened EN-24 steel disc (surface roughness = 0.4-0.5 μm) of diameter 12cm with Rockwell hardness of 57 HRC and a specimen holder. Rotation speed of the disc was kept constant at 2m/s throughout the investigation. Wear test specimens was mounted in a specimen holder. The load on the specimen was applied by placing a load on the opposite side of a fulcrum of the lever attached to the specimen holder. The samples were run

for a period of 25 minutes before calculating their weight loss which was used to find the resultant wear volume. The radius of rotation was fixed at 50 mm. sliding distance for one run comes out to be around 2100 m for this radius. The standard wear test procedure was followed for evaluating the wear rate for different load ranging from 5N to 20 N. The disc surface was cleaned with acetone before each experimental run. All the tests were carried out in dry sliding conditions and at room temperature. Pin specimens were weight both before and after testing on a single pan electrical balance that gave reading to 0.01 mg.

## 3.3 MODELING WITH NEURAL NETWORKS

A three-layer feed forward back propagation neural network was applied as the network structure of the system model. Each node represented an artificial neuron and neurons in the same layer are affected only by neurons in the previous layer. The nodes in the input layer and the output layer, respectively, equal the Eigen value numbers of the input and output patterns, while the nodes in the hidden layer are determined by numerical trial. The Sigmoid function was applied as the transmission function of the hidden layer and the output layer. The schematic view of the model is shown in Fig. 3.3.

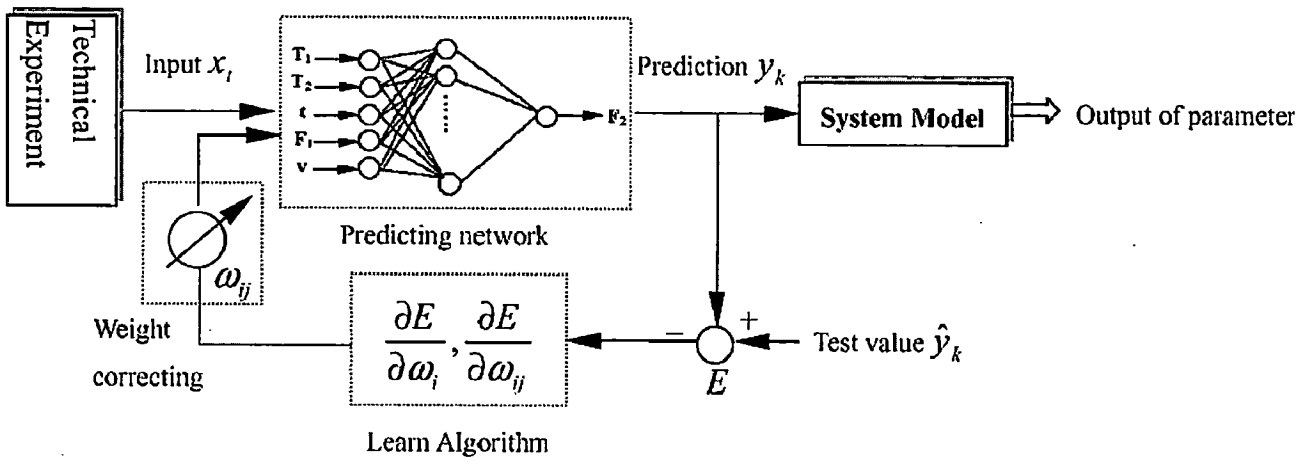


**Figure 3.3** Scheme of modeling the system by ANN

### 3.3.1 DATA SET AND PROCESSING

The inputs to individual ANN nodes must be numerical and fall in the closed interval [0, 1]. Because of this conversion method the normalization technique was used in the proposed ANN according to the following formula:

$$\text{Normalized value} = \frac{\text{inputvalue} - \text{minimum value}}{\text{maximum value-minimum value}}$$

Output values resulted from ANNs are also in the range [0, 1] and converted to their equivalent values based on reverse method of normalization.

### 3.3.2 LEARNING RULES AND TESTING

Neural networks are adaptive statistical devices. This means that they can change iteratively the values of their parameters (i.e., the synaptic weights) as a function of their performance. These changes are made according to the learning rules of gradient descent method. Sigmoid function is the most common activation function in ANN because it combines nearly linear behavior, curvilinear behavior, and nearly constant behavior, depending on the value of the input. The sigmoid function is sometimes called a squashing function, since it takes any real-valued input and returns an output bounded between [0, 1]

$$y = f(x) = \frac{1}{1+e^{-x}}$$



Back propagation neural networks represent a supervised learning method, requiring a large set of complete records, including the target variables. As each observation from the training set is processed through the network, an output value is produced from output nodes. These values are then compared to the actual values of the target variables for this training set observation and the errors (actual-output) are calculated. Normalized root mean square error value (NSE) was used to evaluate the training performance of the ANN

$$\text{NSE} = \sqrt{\frac{\sum(\theta - \theta_0)^2}{\sum \theta^2}}$$

Where $\boldsymbol{\theta}$ is the experimental value and $\theta_0$ represents the predicted output value.

It is important to evaluate the performance of the ANN model. This is done by separating the data into two sets: the training set and the testing set. The parameters (i.e., the value of the synaptic weights) of the network are computed using the training set. When reaching the error goal the learning process is stopped and the network is evaluated with the data from the testing set.

# Chapter 4

# RESULTS AND DISCUSSION

## 4.1 MICROSTRUCTURAL FEATURES

Optical micrographs were taken at three different locations for both alloys (Al-Graphite and Al-Si-Pb). The micrographs for aluminum-8wt%Graphite are shown in the Fig 4.1 and 4.2

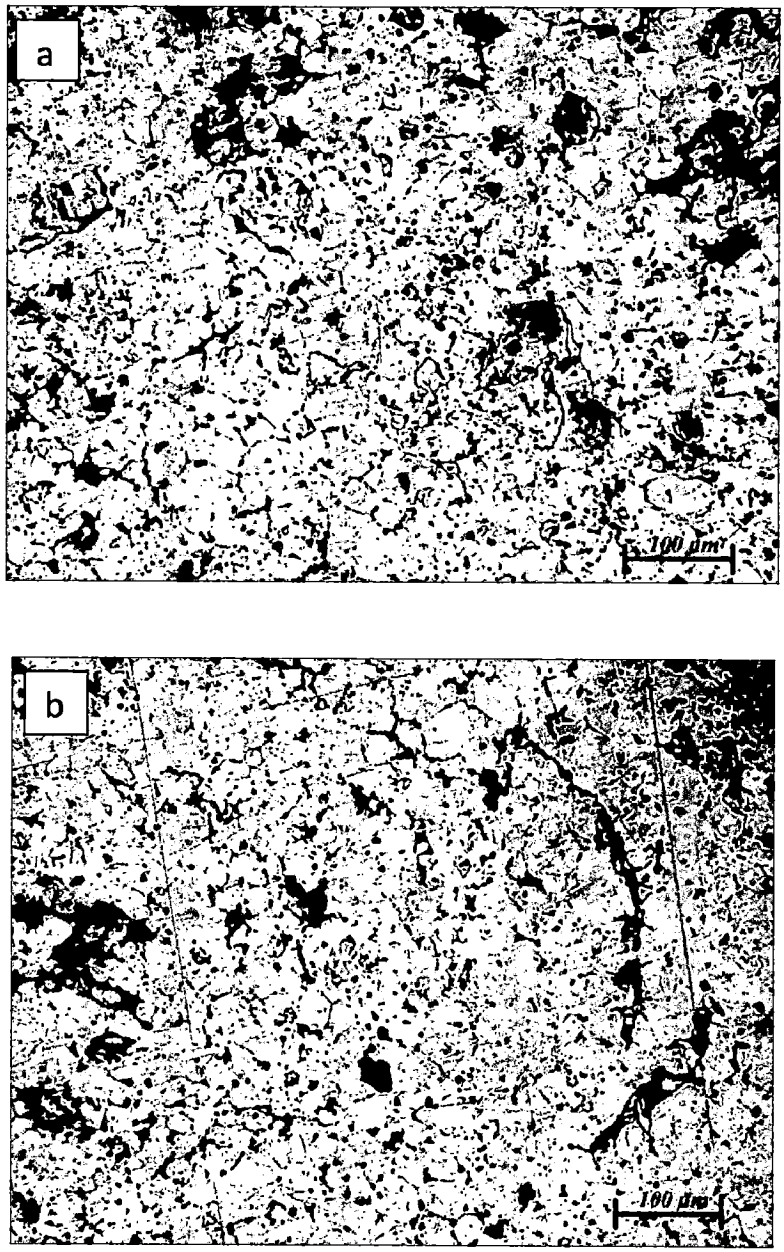


**Figure 4.1** Optical microstructure of spray deposited Al -8Graphite alloy showing (a) top, (b) middle.

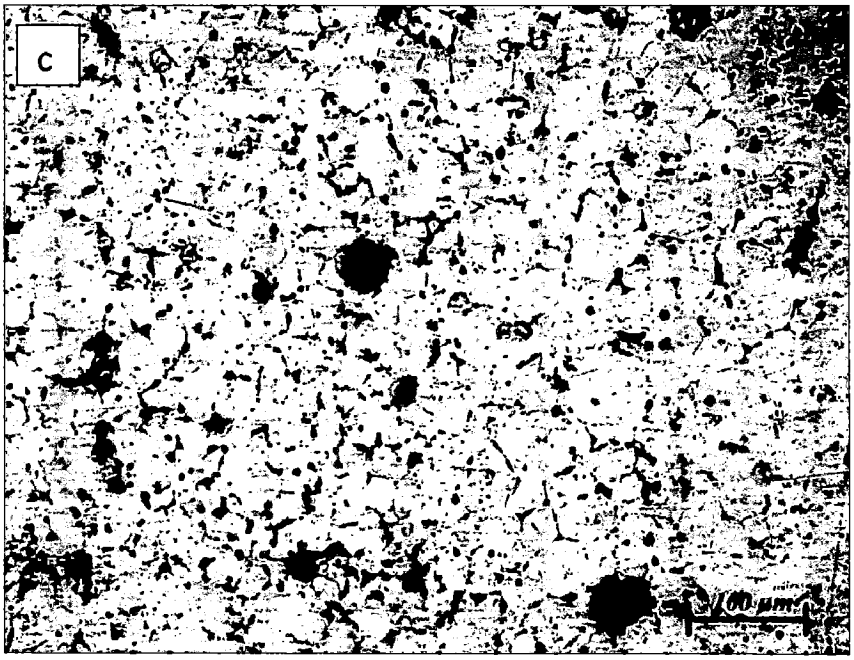


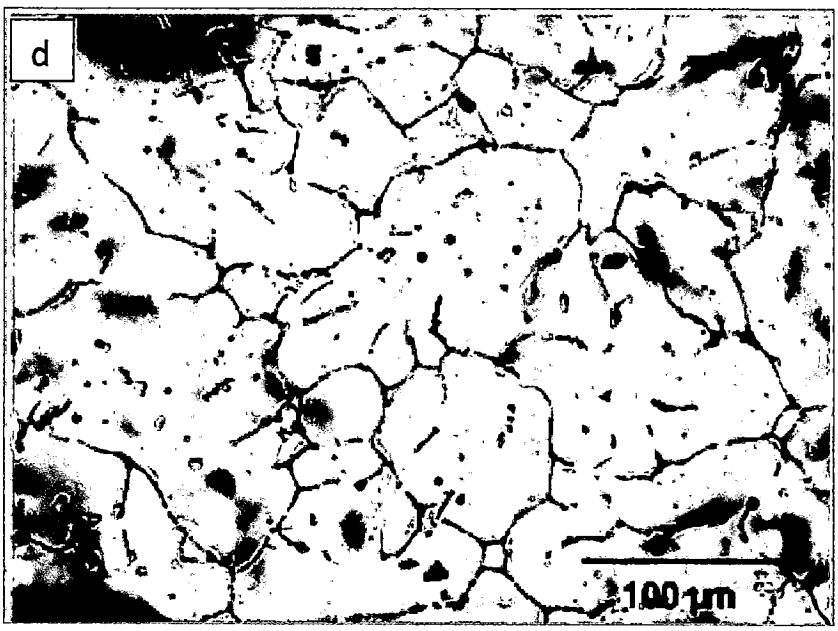


**Figure 4.2** Optical microstructure of spray deposited Al – 8Graphite alloy showing (c) bottom and (d) pure aluminum.

The microstructure for Aluminum-Silicon-Lead is shown in Fig 4.3, 4.4 and 4.5 for top, middle and bottom samples.

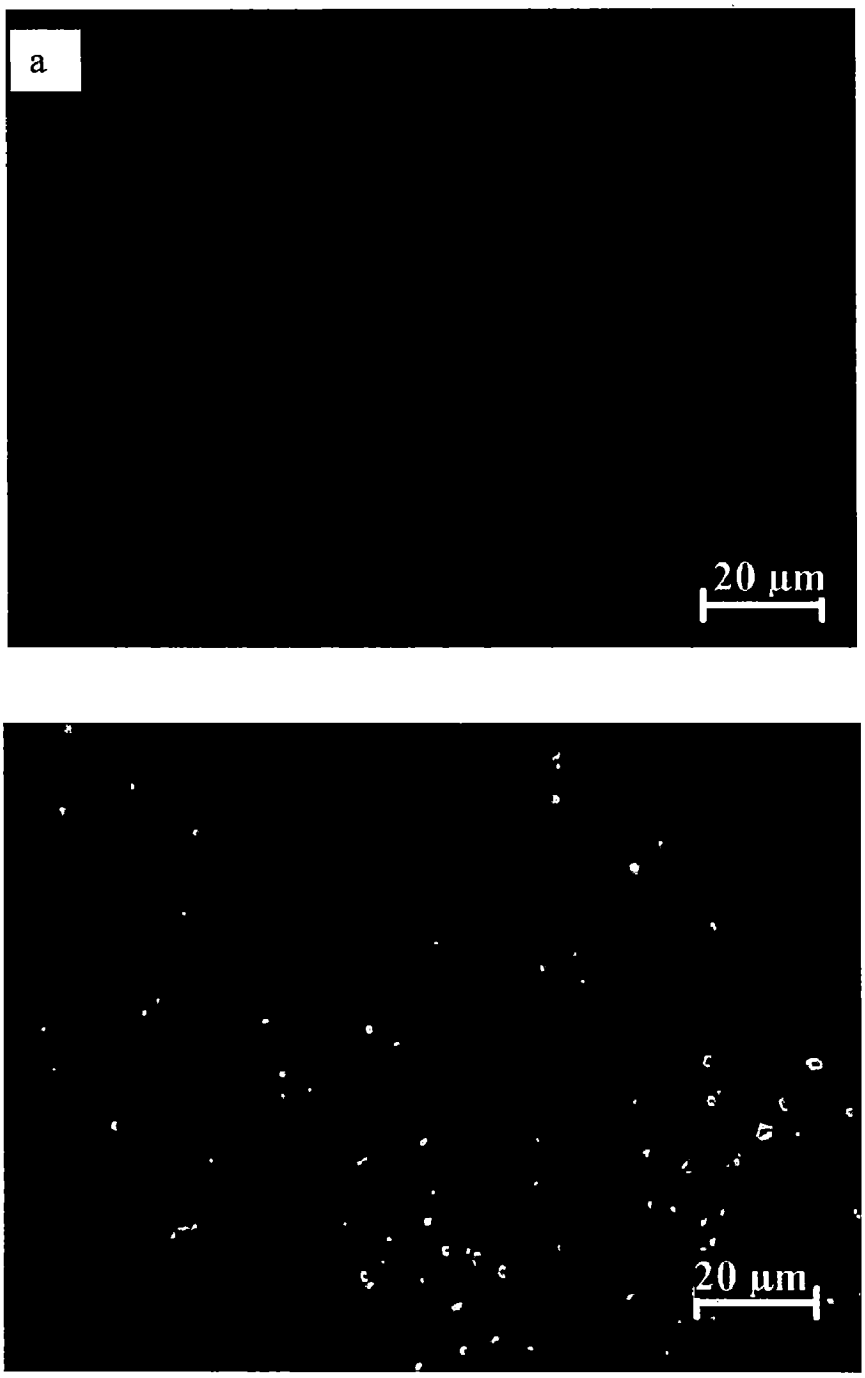


**Figure 4.3** Optical microstructure of spray deposited Al-6Si-10Pb alloy showing (a) top.

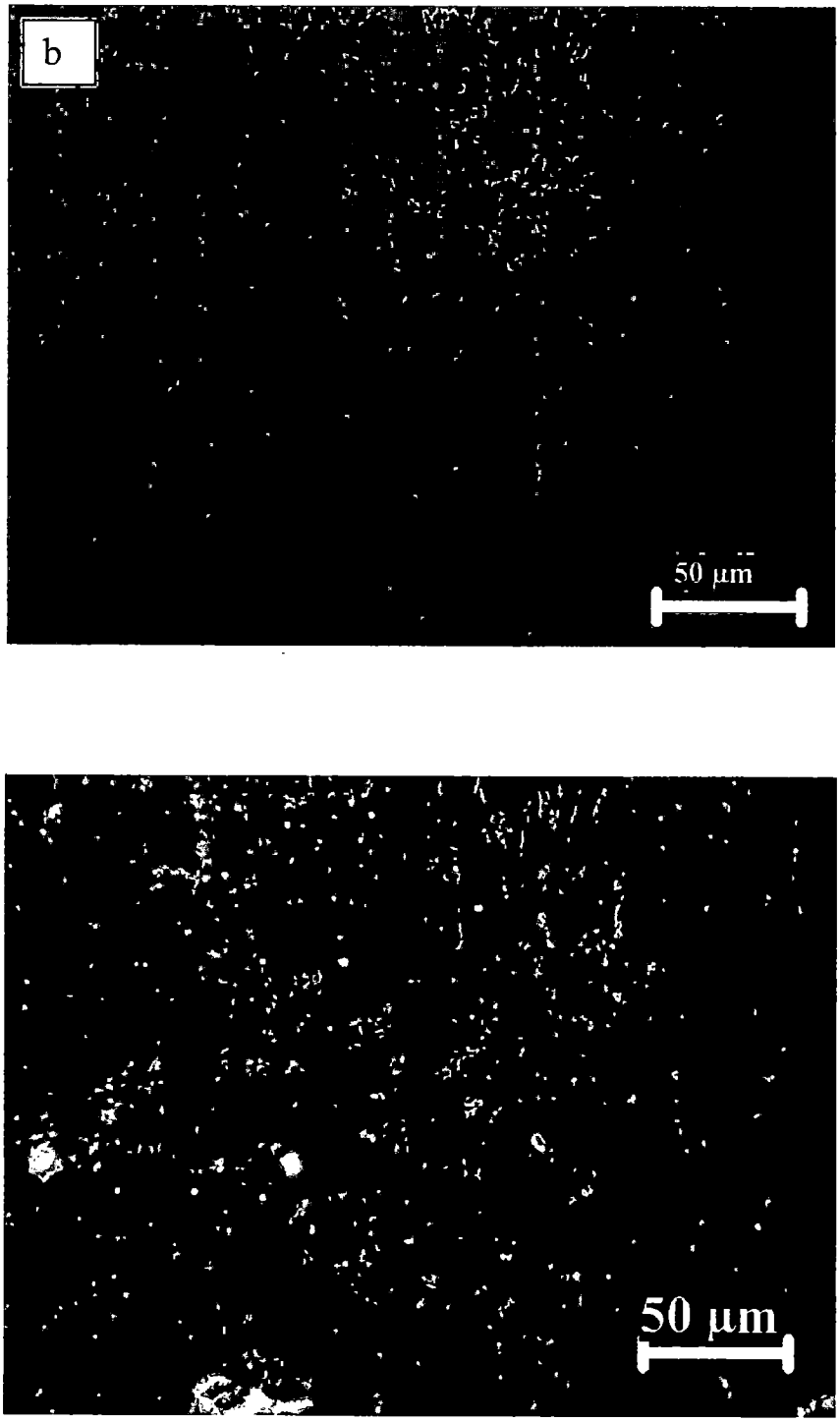


**Figure 4.4** Optical microstructure of spray deposited Al-6Si-10Pb alloy showing (b) middle.

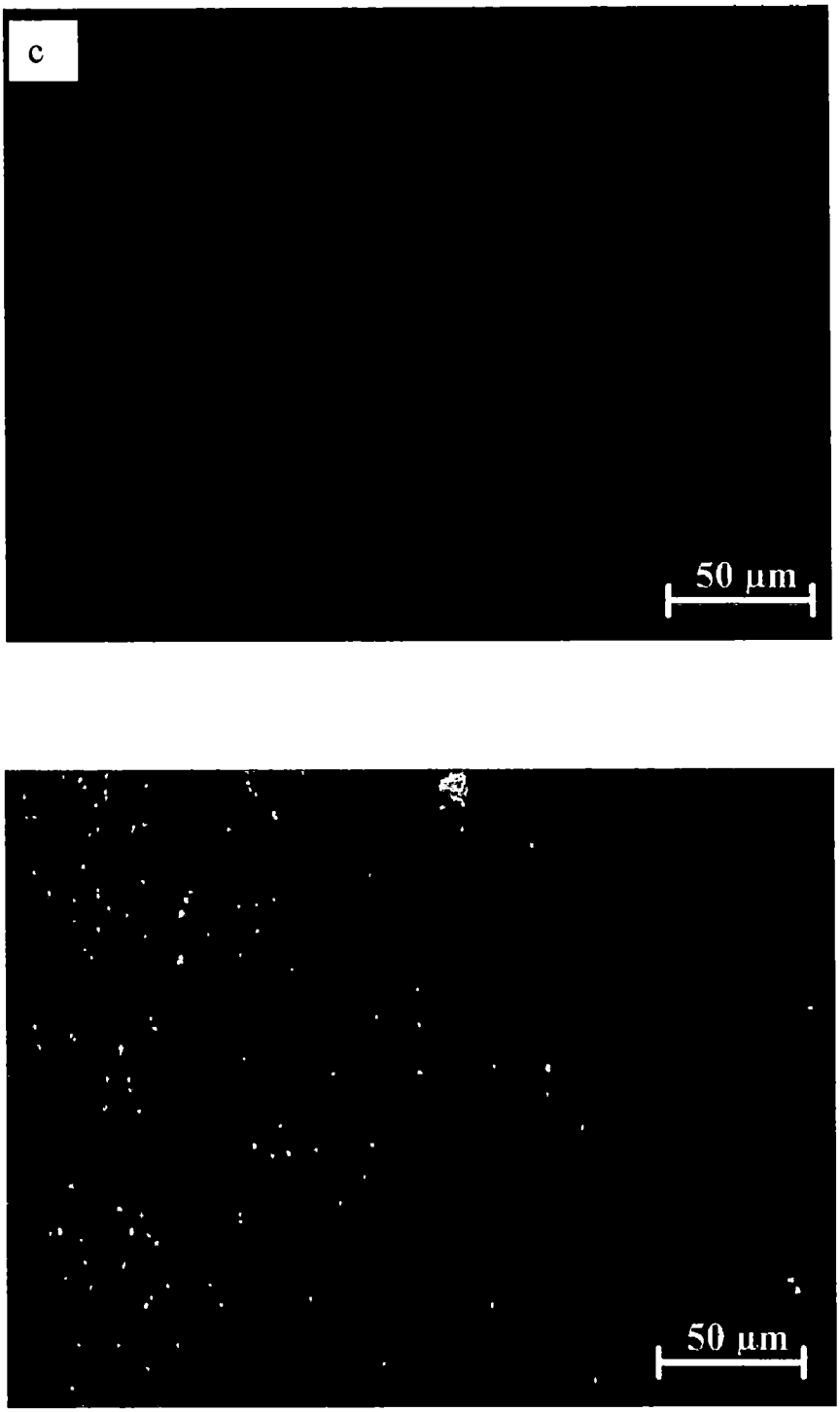


**Figure 4.5** Optical microstructure of spray deposited Al-6Si-10Pb alloy showing (c) bottom.

Figures 4.1 to 4.5 shows the optical microstructure of Al-graphite, pure aluminum and Al-Si-Pb. Large grains were observed in unreinforced pure Al. In unreinforced pure Al, there are well defined grain boundaries and in Al–8 wt. % Graphite composite, grain boundaries are not well defined but rather poorly delineated and irregularly shaped or curved. Grey color in microstructure represents graphite. It can be seen that graphite distribution is almost uniform throughout the aluminum phase. Grain boundaries are clearly visible in Al-Si-Pb alloy. Fig. 4.3 to 4.5 show the Pb distribution in the equi-axed region of Al-Si-Pb preform in the as-polished condition. Equiaxed grains of primary Al were observed and Si was present within these grains and along the grain boundaries. The average Al grain size is about 35 μm. Dark gray color in microstructure represents Si phase. White color represents the Pb phase. It can be seen that the Pb distribution is almost uniform throughout the aluminum phase. The Pb particles are located mainly at the grain boundaries. It can be seen that the grains are clearly visible in middle and bottom region. Figure 4.6 shows the SEM micrographs of Al-8Graphite and Al-6Si-10Pb at central region of deposit. In Al-Si-Pb the white phase is Pb, and dark gray phase is Si (are revealed by EDAX analysis as shown in Fig. 4.8) which is distributed along grain boundaries and inside the Al grains. Atomization of the melt from the temperature above the liquid immiscibility boundary initially results in separation of Al and Pb-rich liquid during solidification of droplets. A high cooling rate associated with solidification of droplets minimizes coarsening of Pb-rich droplets. Once the temperature of the melt approaches to the monotectic temperature of the alloy on the deposition surface, the primary Al phase nucleates and grows. The Pb - rich liquid further breaks into still smaller size droplets on the deposition surface. In this case, the morphology of Pb particles depends upon the solidification rate of Pb rich droplets. A slow cooling rate results in spheroidization of the Pb -rich droplets whereas high cooling rate promotes their irregular shape. As a consequence of this, the morphology of lead particles varies in different region of the deposits that undergoes a variation in cooling rate. Solidification of the Pb-rich liquid is further influenced by the presence of Si particles in this alloy. The Si phase solidifies at an early stage due to its high freezing temperature. Thus, the particles of Si often provide nucleation sites for further crystallization of low melting Pb phase. Due to a good wettability between Si and Pb rich liquid, solidification of Pb takes place around the existing Si particles. Maximum amount of lead is on the grain boundaries. In Al-Graphite the gray phase is graphite (revealed by EDAX analysis as shown in Fig. 4.7).

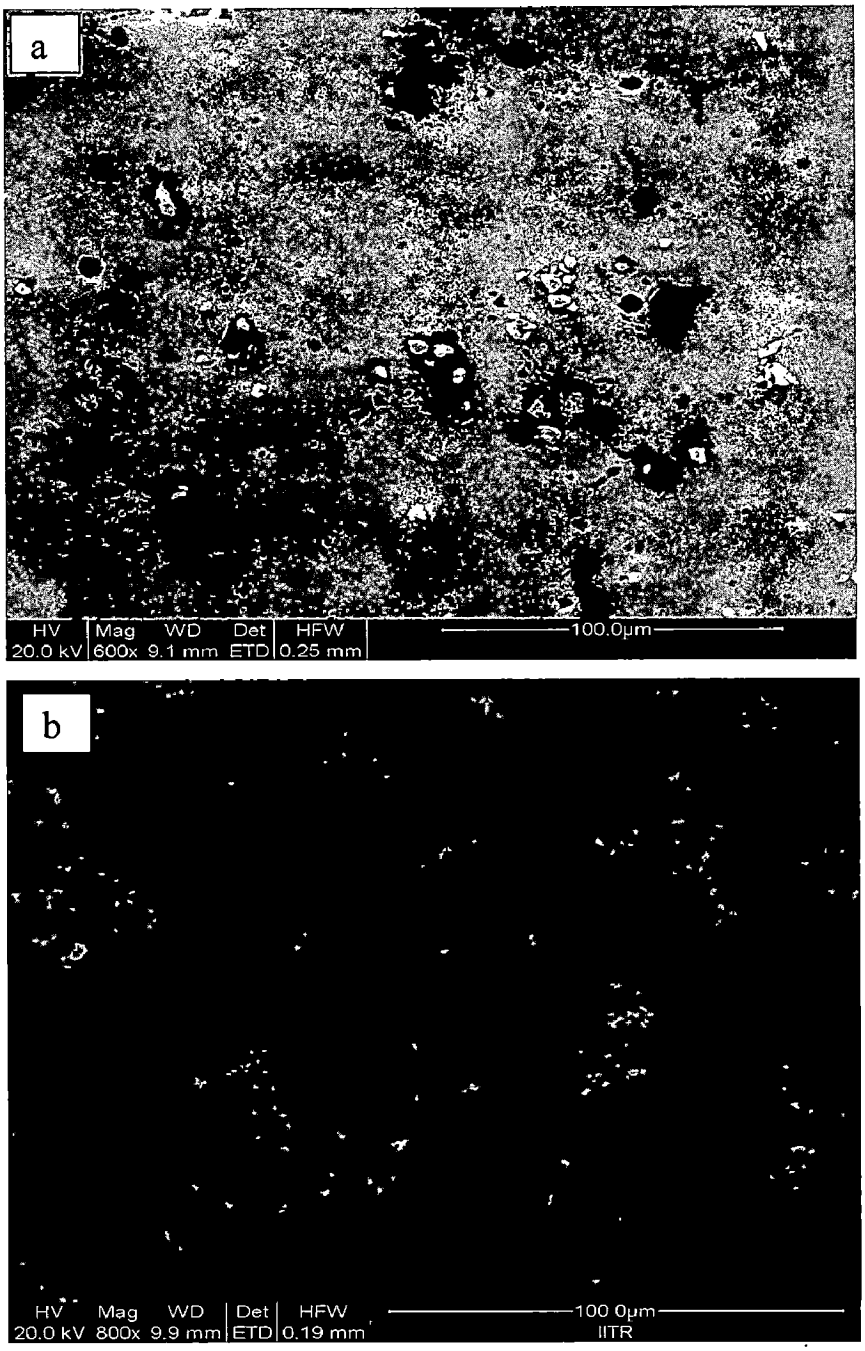


**Figure 4.6** SEM micrographs of (a) Aluminum-graphite (b) Al-Si-Pb.

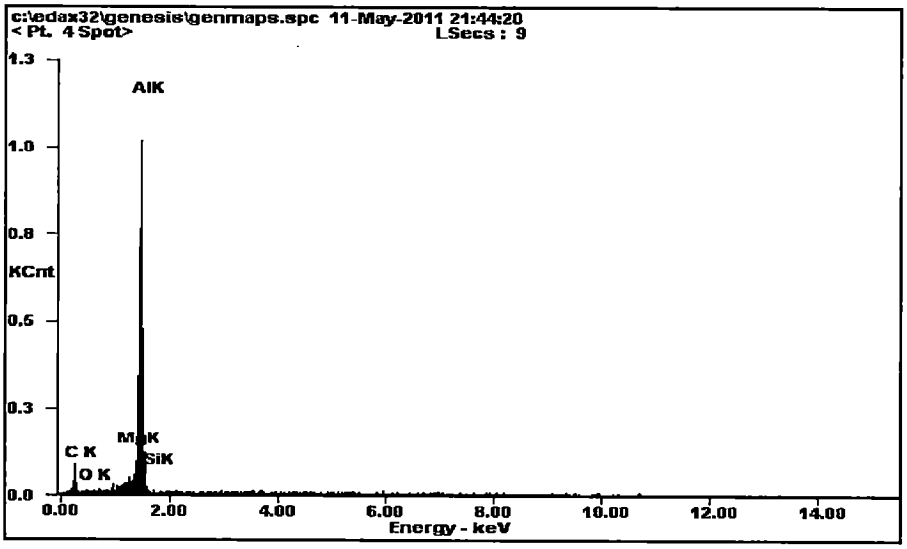


| | | |
|---|---|---|
| ***CK*** | 44.38 | 63.82 |
| ***OK*** | 01.03 | 01.11 |
| ***MgK*** | 01.84 | 01.31 |
| ***AlK*** | 52.67 | 33.72 |
| ***SiK*** | 00.07 | 00.04 |
| ***Matrix*** | Correction | ZAF |

**Figure 4.7** EDAX Spectrum of Al-graphite.

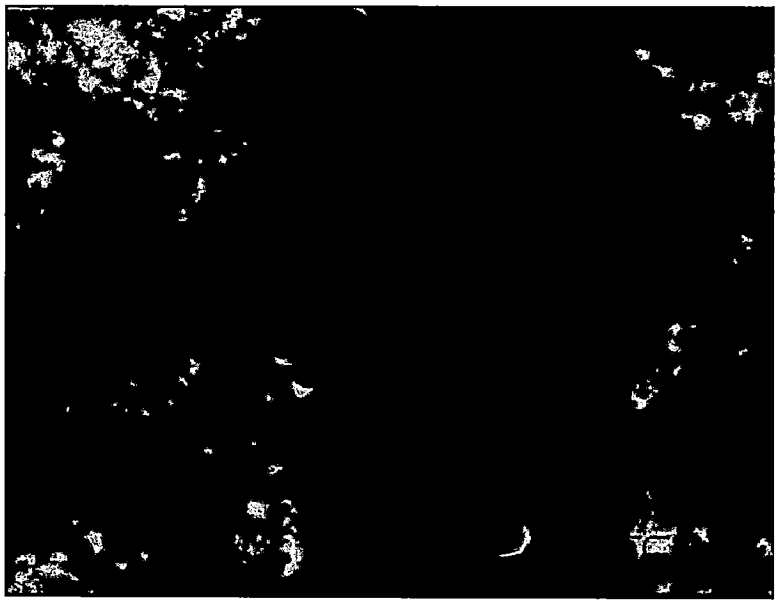

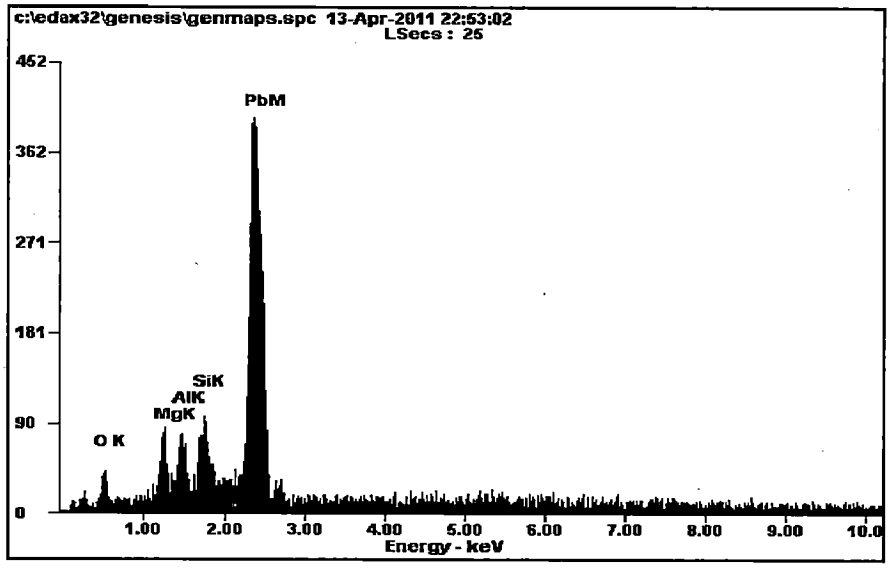


| *Element* | *Wt%* | *At%* |
|---|---|---|
| *OK* | 06.42 | 30.08 |
| *MgK* | 05.35 | 16.48 |
| *AlK* | 04.98 | 13.83 |
| *SiK* | 04.12 | 10.99 |
| *PbL* | 79.13 | 28.62 |
| *Matrix* | Correction | ZAF |

**Figure 4.8** EDAX Spectrum of Al-Si-Pb.

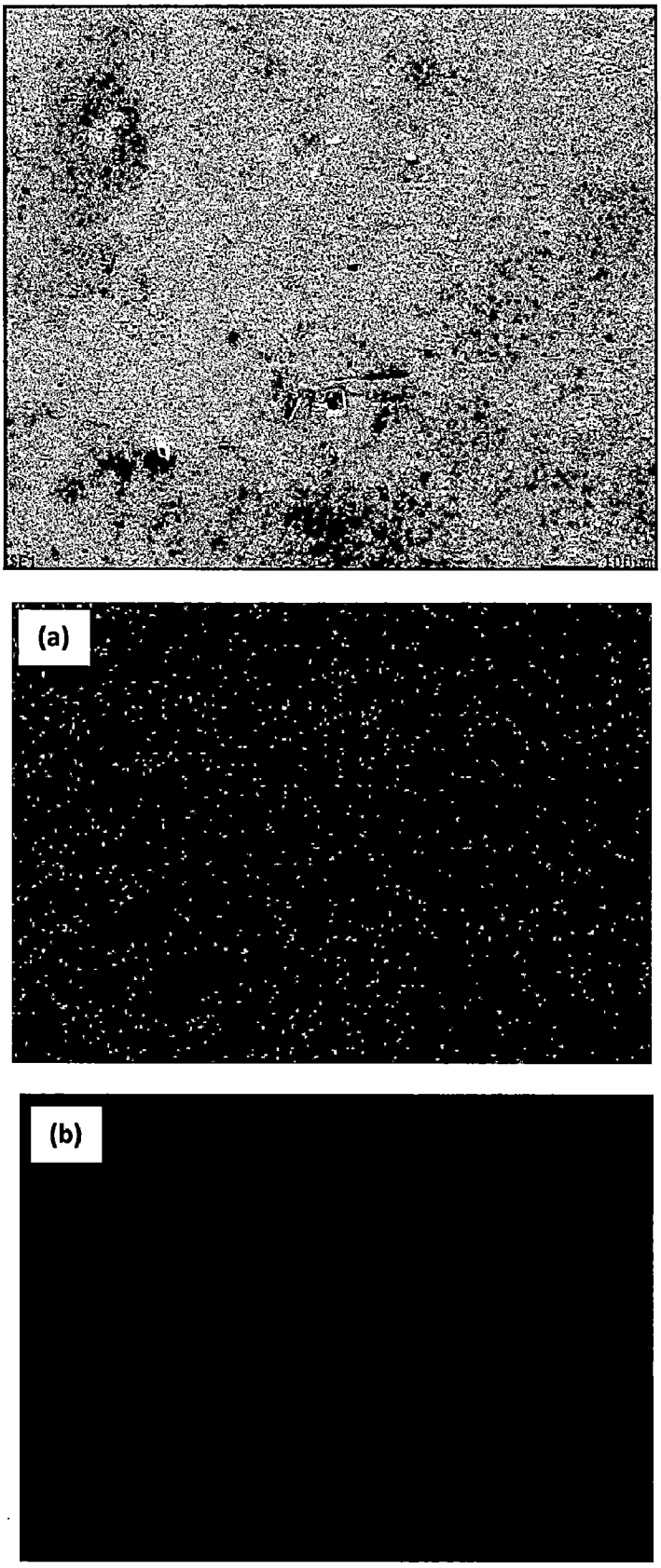


**Figure 4.9** Color dot maps of two elements: (a) Al; (b) graphite in Al-8graphite spray deposit

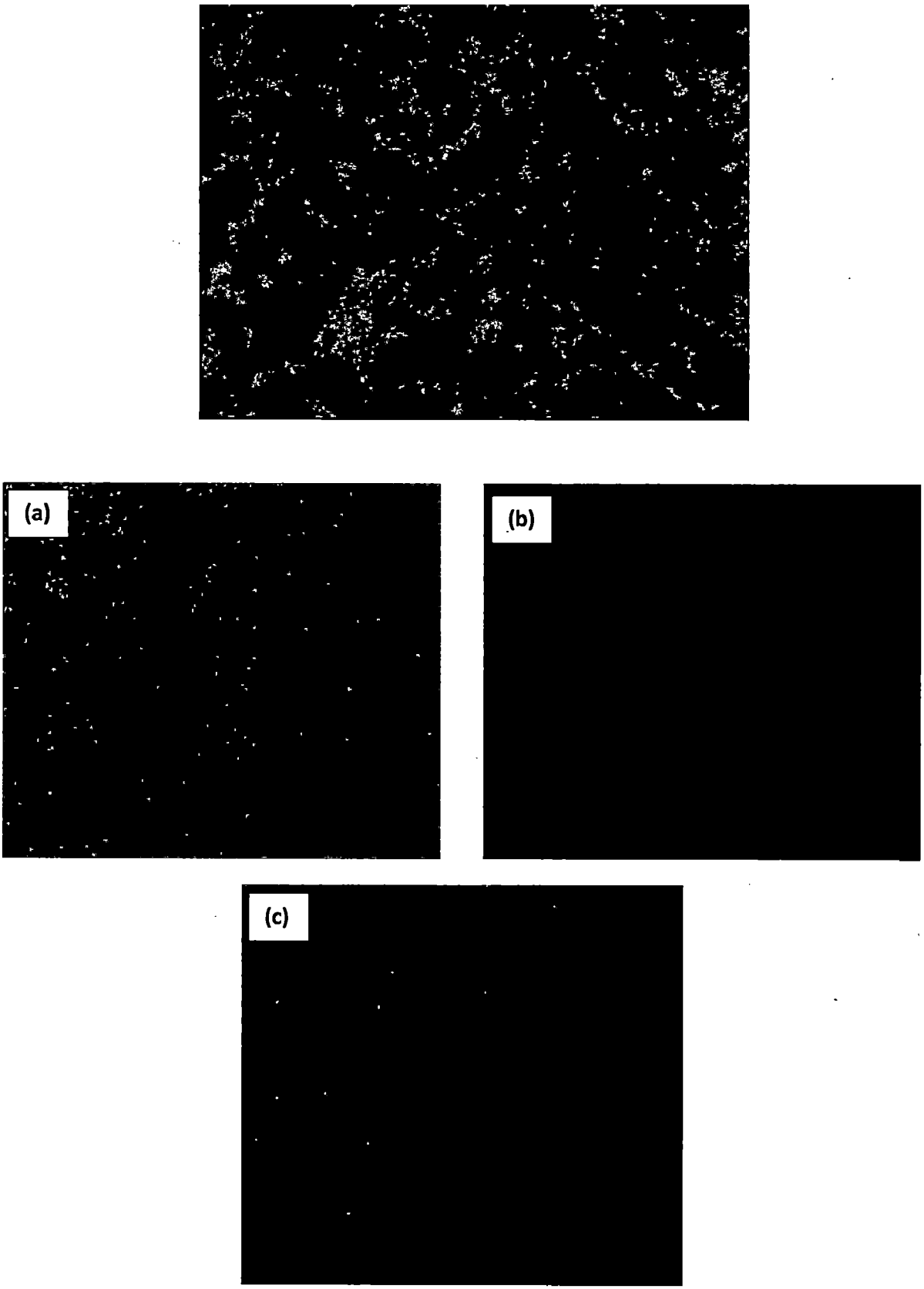


**Figure 4.10** Color dot maps of all three elements: (a) Al; (b) Si and (c) Pb in the Al-6Si-10Pb spray deposit

Color dot maps of Al and Graphite in Al-8Graphite alloy are shown in Fig. 4.9 which represents a uniform distribution of Aluminum and Graphite elements in the spray deposit.

Color dot maps of Al, Si and Pb distribution in Al-6Si-10Pb alloy are shown in Fig. 4.10 which represents a uniform distribution of these elements in the spray deposit. The refined equi-axed grain structure is formed as a consequences of the following: (1) high velocity impacting of the solid or semi-solid droplets on to the top surface of the preform, resulting in dendritic "blocks" immersing in the solute-poor liquid films; (2) coarsening of the rapidly solidified dendritic structure in the "blocks" leading to equi-axed grains; (3) solidification of the solute-poor liquid films, retarding grain boundary migration, resulting in the refined grain structure and low segregation level. The presence of Pb particles at the grain boundaries indicates that a liquid film network existed in the preform during processing because the rearrangement and coalescence of liquid Pb during deposition must rely on the liquid Al-Si because Pb has limited solubility in liquid Al at the temperature when the semi-solid state is maintained and has close-to-zero solubility in the solid Al the refinement of the microstructure, caused by grain boundary drag effect induced by the Pb particles.

## 4.2 HARDNESS

Hardness testing was conducted on the spray formed samples using Vickers hardness testing machine.

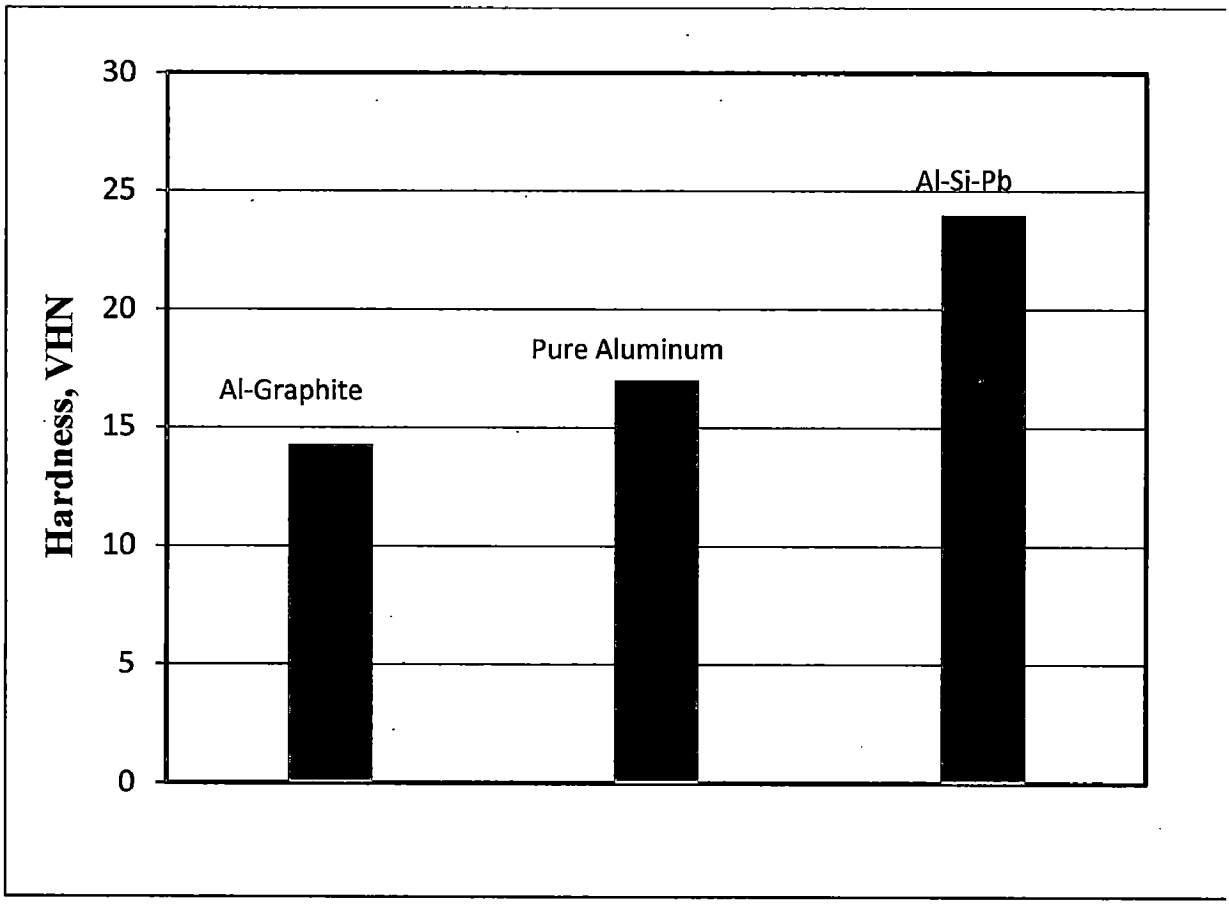


**Figure 4.11** Comparison of variation in hardness for Al-graphite, pure aluminum and Al-6Si-10Pb.

The variation in hardness for Al-graphite, pure aluminum and Al-Si-Pb is shown in figure 4.11. Hardness of Al-Si-Pb is more than that of Al-graphite alloy. The main reason is: the ultra-fine and homogeneous lead phase distributed in the aluminum matrix by spray forming. The second is that the lead crystallite grain size still is in the nanometer range after spray forming, and also that there is amorphous areas distribution in the aluminum matrix.

Figure 4.12 shows the hardness of deposit as a function of distance from bottom to top (height) of the preform for both Al-graphite and Al-Si-Pb alloy. The hardness was found almost constant at all the heights of the perform.

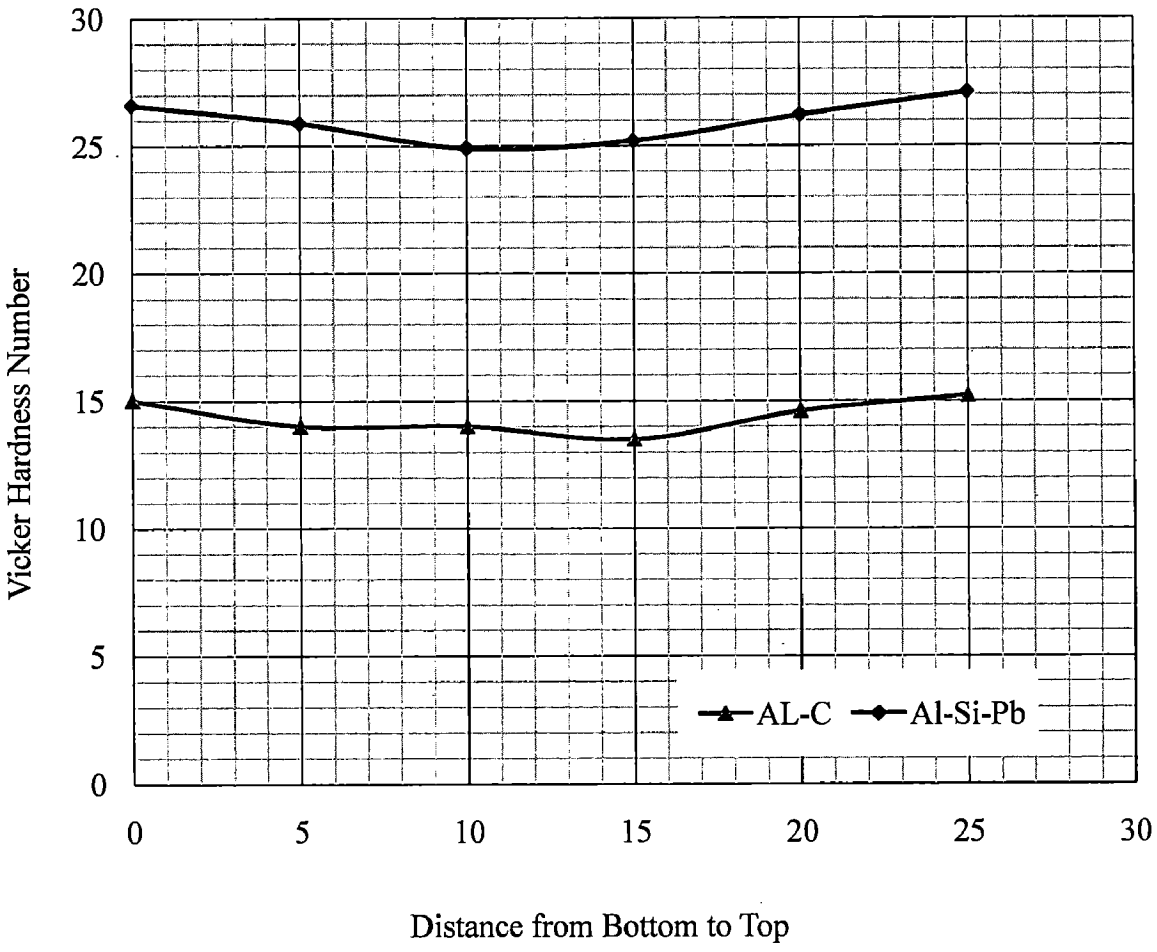


**Figure 4.12** Variation in hardness with distance from bottom to top at the centre of the deposit.

## 4.3 EFFECT OF ROLLING

A sample of size 20 mm × 15 mm was taken from the spray deposited Al–8wt% graphite strip for the study of the rolling behavior. This had a thickness of 4.8 ± 0.5 mm. The spray deposited Al–graphite strip samples were rolled at room temperature on two-high rolling mill. The cold rolling was performed on two-high mill with rolls of 110 mm in diameter. The nominal rolling speed was 8rpm. The strips were rolled to various thickness deformations in the range 20–80%. More cracks were observed in 80% deformation sample. The micrographs for different rolling conditions are shown in Fig. 4.13.

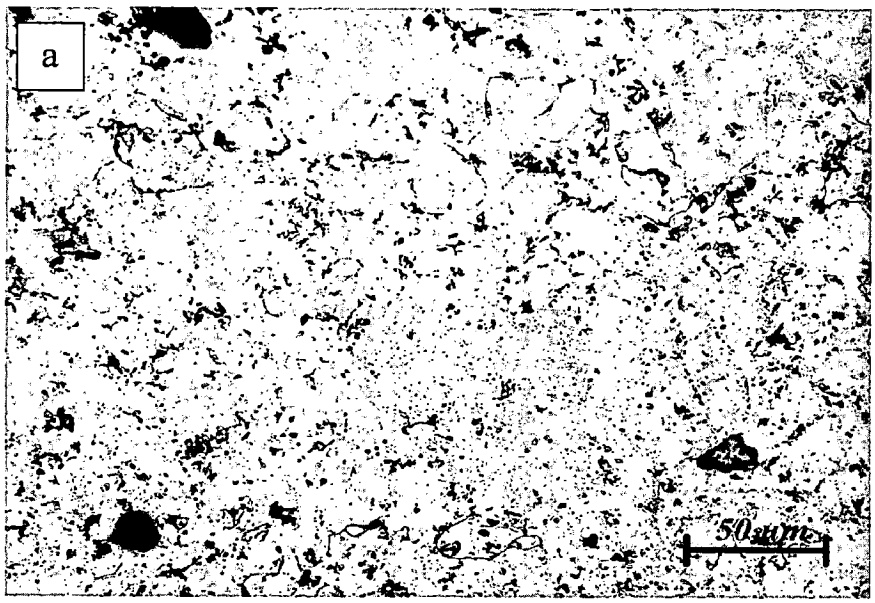


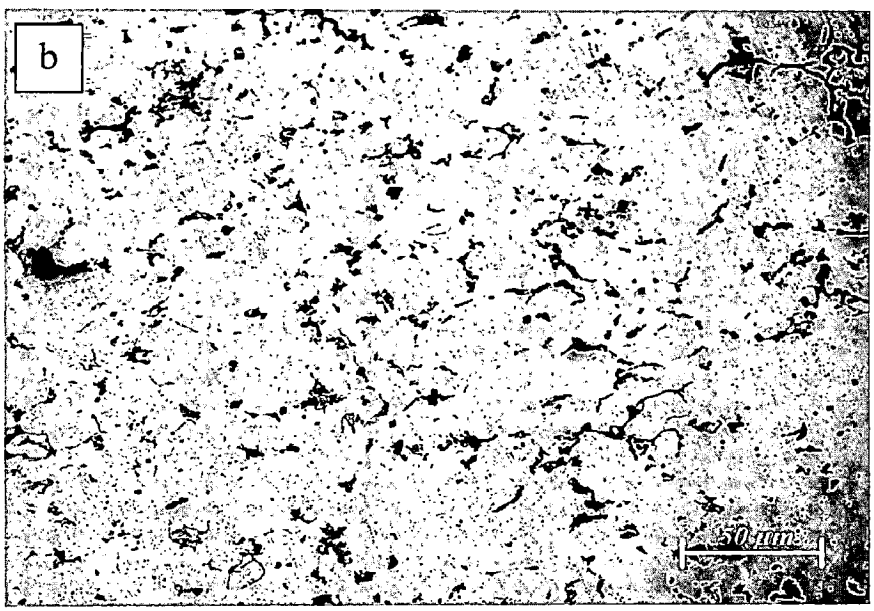

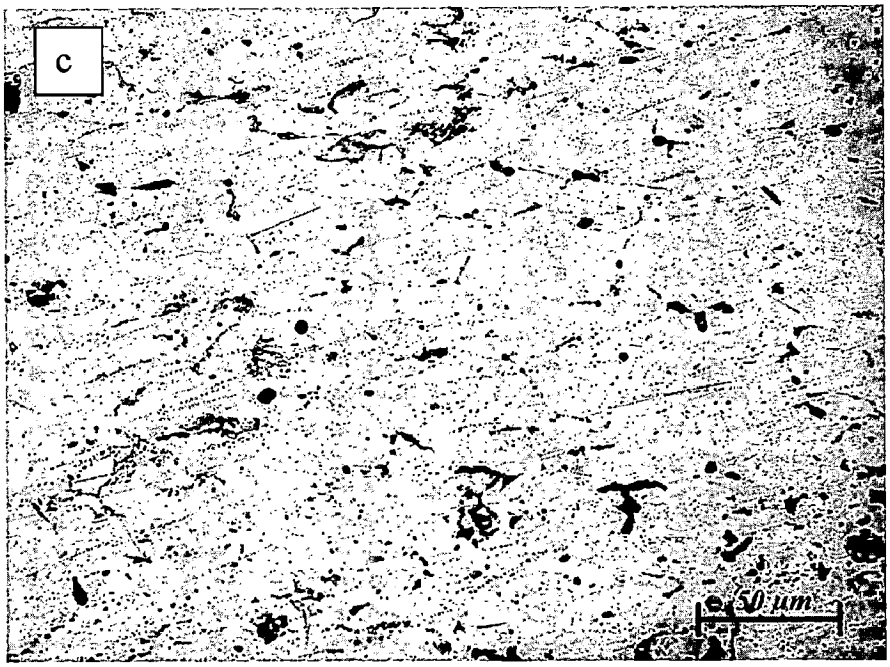


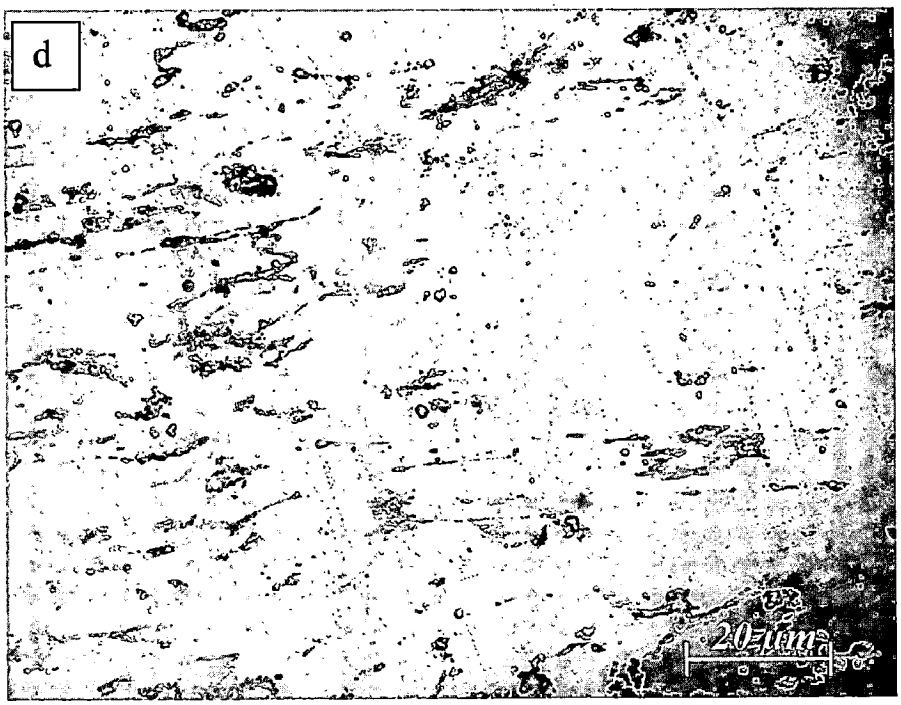


**Figure 4.13** Optical Micrograph after (a) 20% (b) 40% (c) 60% (d) 80% reduction in thickness

The bright phase corresponds to aluminum, whereas the dark grey phase represents graphite and the small black spots represents residual porosity. During rolling, both densification and deformation in the Al–graphite deposit take place simultaneously. In the initial stages of rolling (i.e. about 20% thickness deformation), the metal flow in the Al–graphite deposit is mainly in the thickness direction resulting in the removal of porosity by rearrangement and restacking of spray deposited particles. Beyond this, plastic deformation becomes the predominant mechanism of densification during rolling. As a result the pores are removed by a process involving pore elongation in the direction of rolling followed by fragmentation into several smaller size pores. This process of elongation and fragmentation of pores continue with rolling. Figure 4.14 shows the SEM micrographs of spray formed Al-graphite alloy at different rolling conditions.

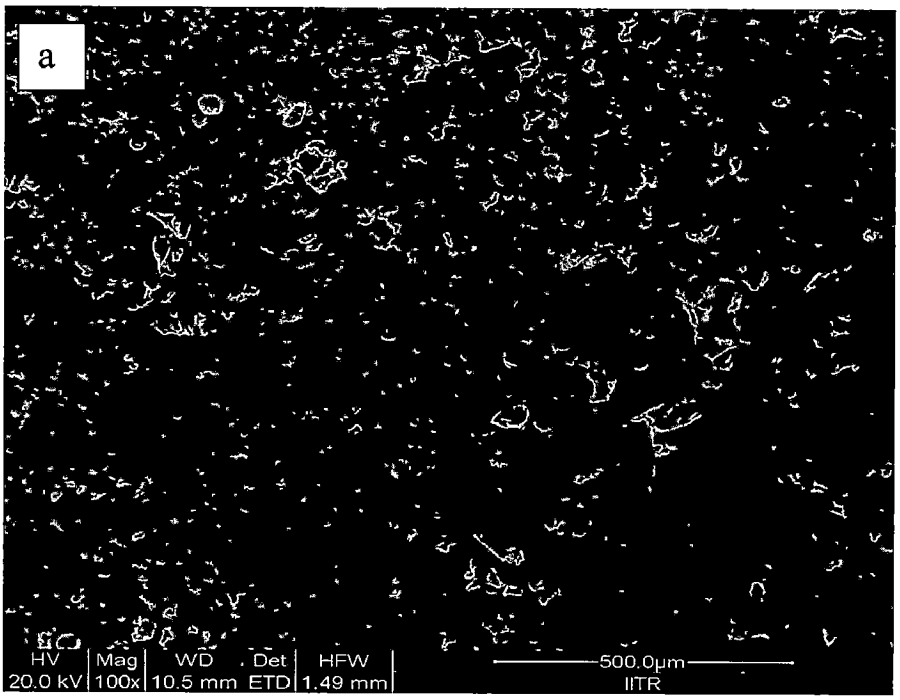

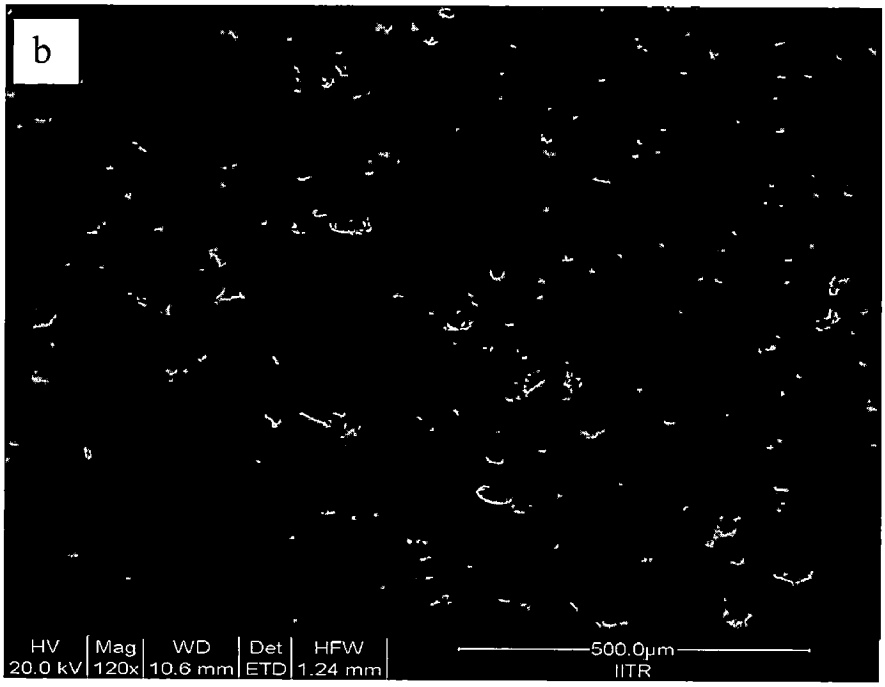
b
HV
20.0 kV
Mag
120x
WD
10.6 mm
Det
ETD
HFW
1.24 mm
500.0µm
IITR

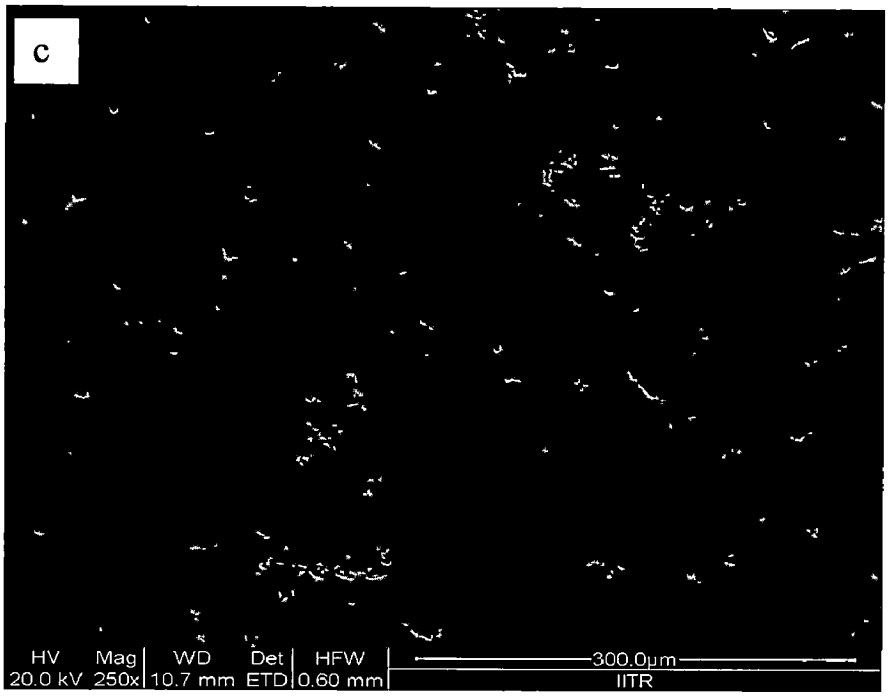
c
HV
20.0 kV
Mag
250x
WD
10.7 mm
Det
ETD
HFW
0.60 mm
300.0µm
IITR

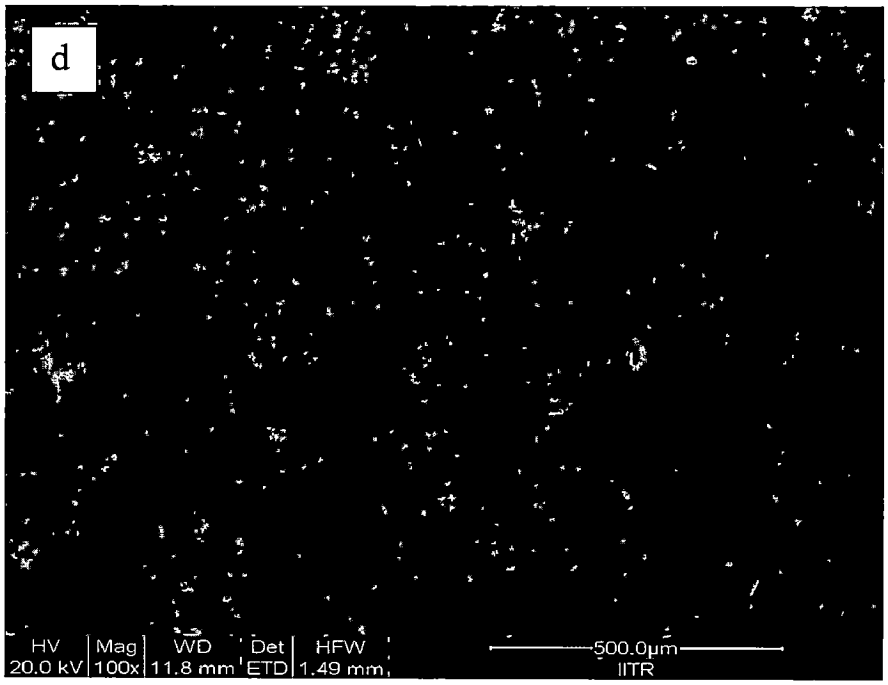


**Figure 4.14** SEM micrographs after (a) 20% (b) 40% (c) 60% (d) 80% reduction in thickness.

Fig. 4.15 to 4.18 shows the EDAX spectrums with micrographs of the analyzed region for Al-graphite spray formed alloy at different rolling conditions. EDAX analysis of black and grey regions of the micrographs gives Al, graphite peaks and these two regions are shown.

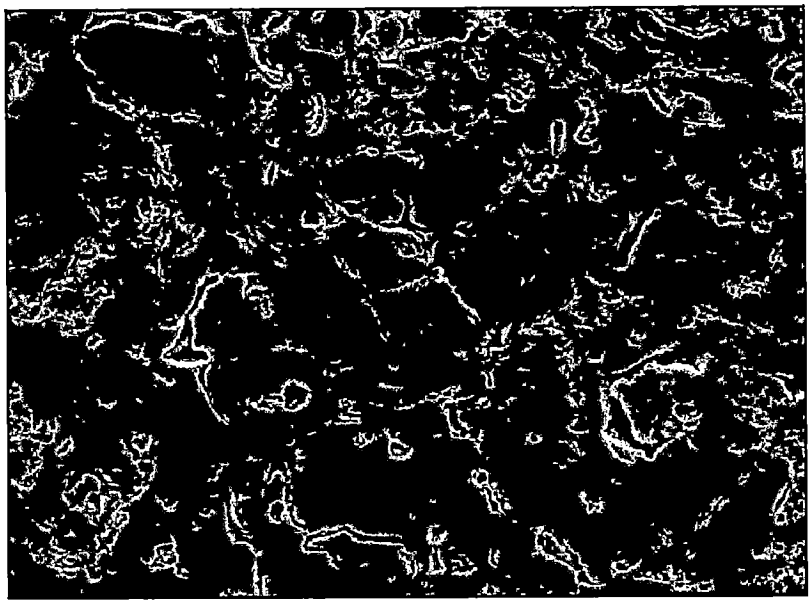

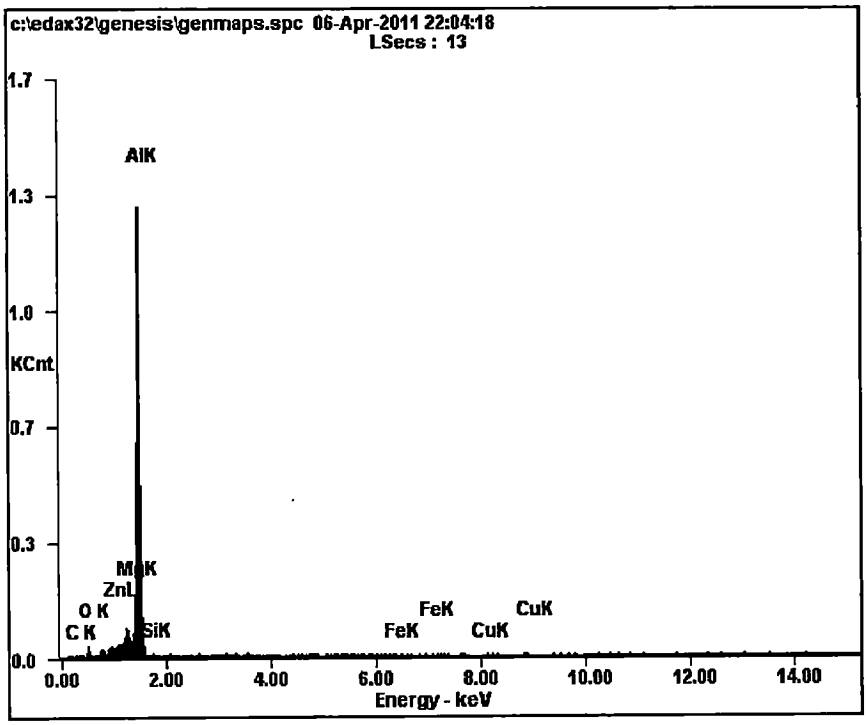


| Element | Wt% | At% |
|---|---|---|
| CK | 01.96 | 04. |
| OK | 03.91 | 06. |
| ZnL | 03.05 | 01. |
| MgK | 04.56 | 04. |
| AlK | 85.44 | 82. |
| SiK | 00.76 | 00. |
| FeK | 00.33 | 00. |
| CuK | 00.00 | 00. |
| Matrix | Correction | ZAI |

**Figure 4.15** EDAX Spectrum of Al-Graphite after 20% reduction in thickness.

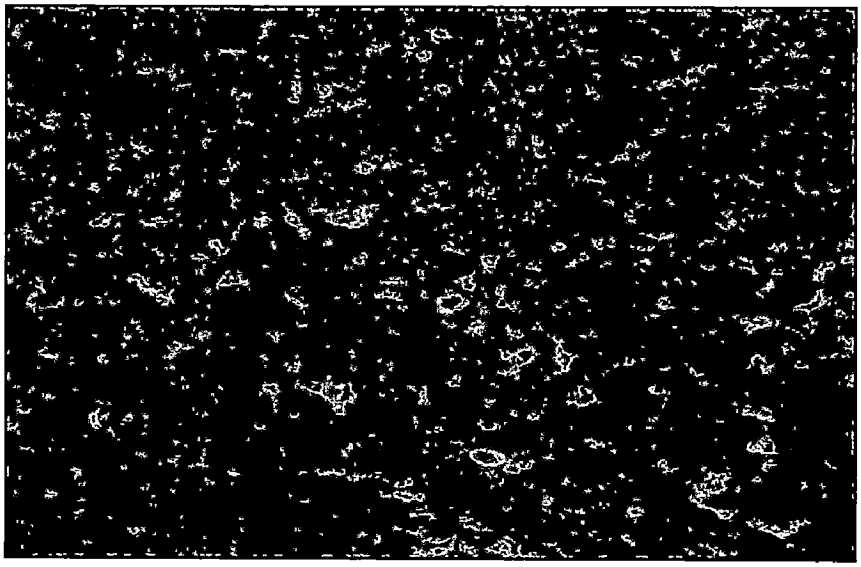

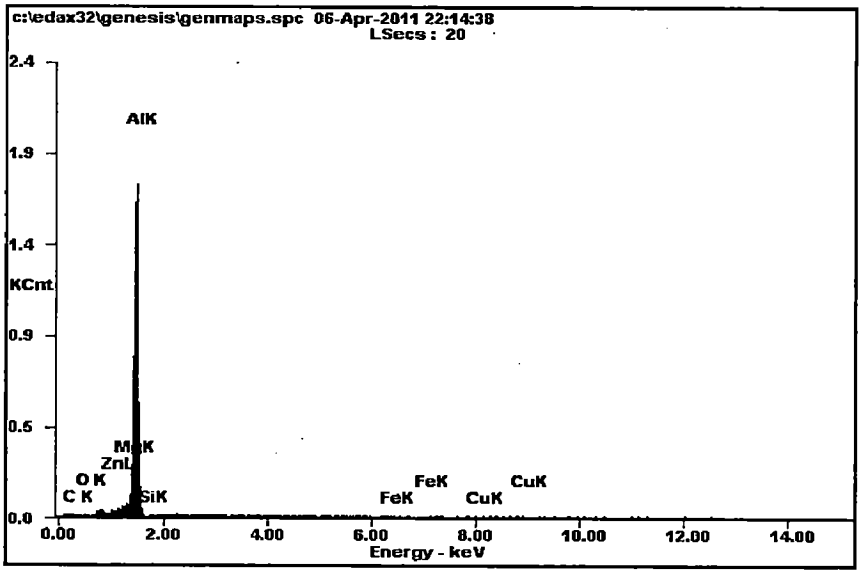


| *Element* | *Wt%* | *At%* |
|---|---|---|
| ***CK*** | 04.14 | 08.88 |
| ***AlK*** | 89.72 | 85.77 |
| ***Matrix*** | Correction | ZAF |

**Figure 4.16** EDAX Spectrum of Al-Graphite after 40% reduction in thickness.

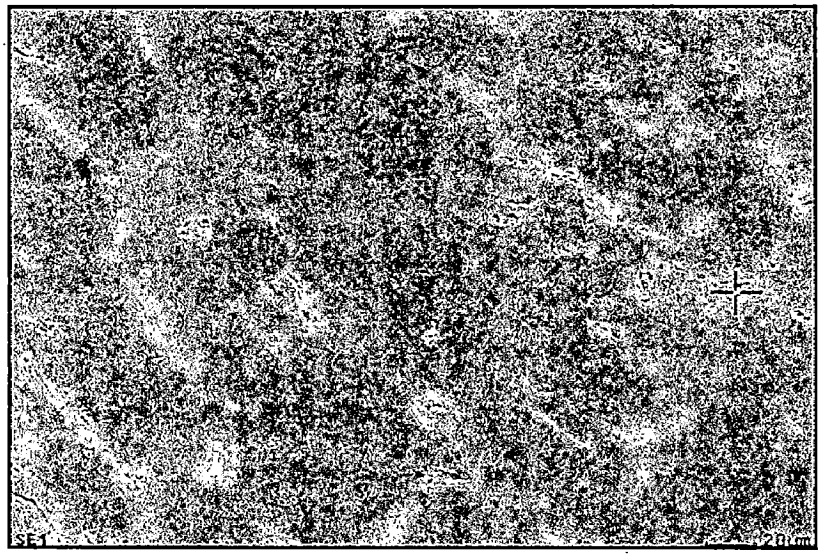

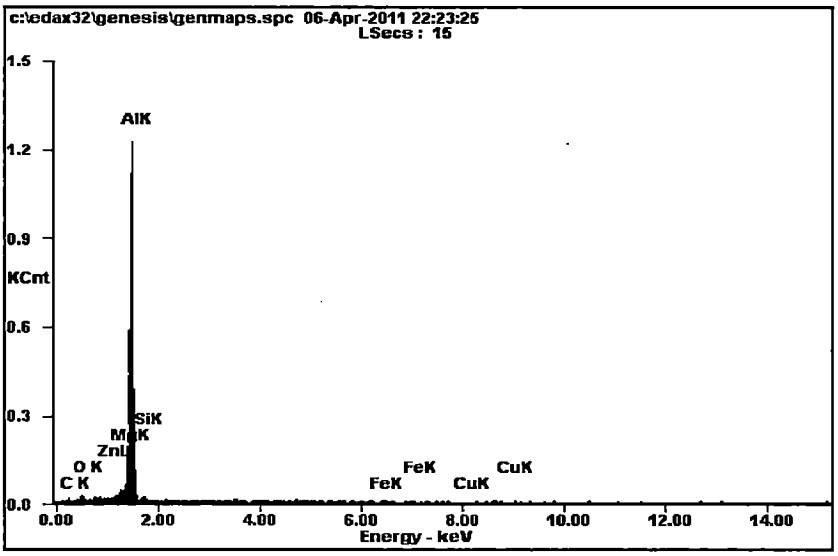


| *Element* | *Wt%* | *At%* |
|---|---|---|
| ***CK*** | 07.60 | 15.14 |
| ***AlK*** | 79.66 | 70.66 |
| ***Matrix*** | Correction | ZAF |

**Figure 4.17** EDAX Spectrum of Al-Graphite after 60% reduction in thickness.

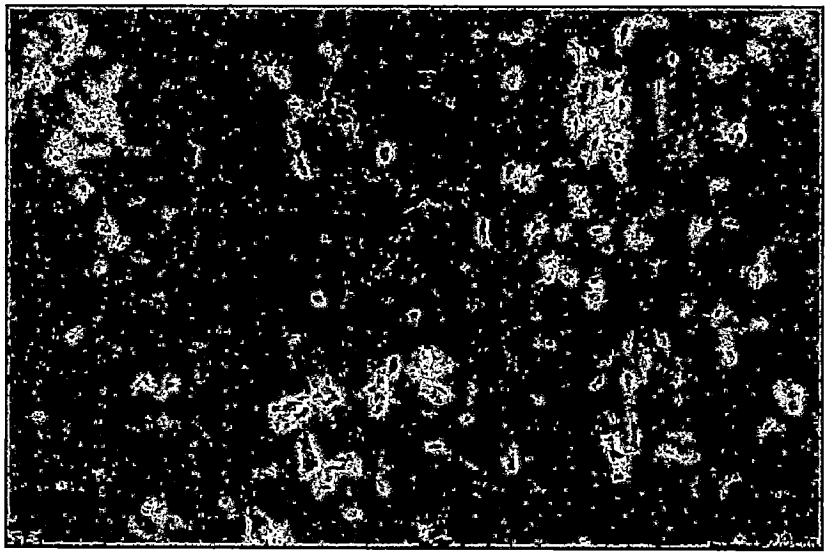

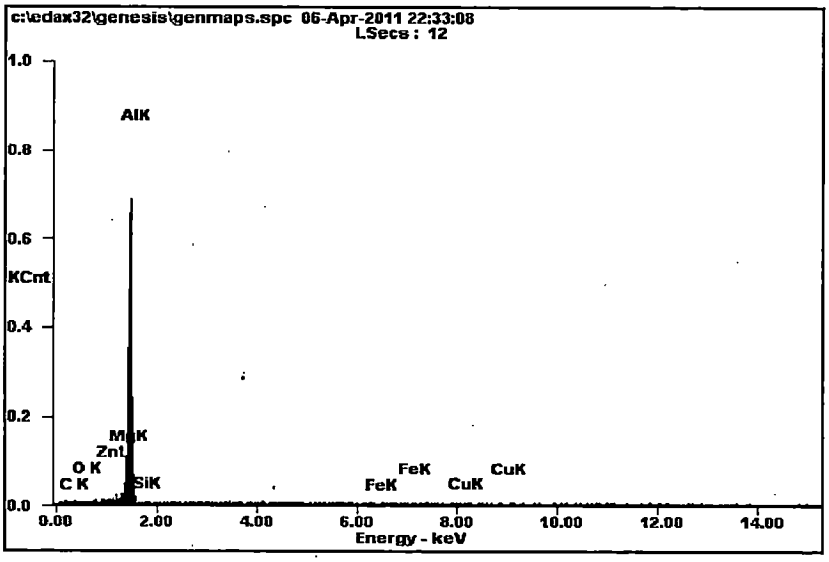


| *Element* | *Wt%* | *At%* |
|---|---|---|
| ***CK*** | 00.00 | 00.00 |
| ***AlK*** | 96.51 | 96.37 |
| ***Matrix*** | Correction | ZAF |

**Figure 4.18** EDAX Spectrum of Al-Graphite after 80% reduction in thickness.

## 4.4 WEAR PROPERTIES

The wear test is conducted at room temperature for constant sliding velocity of 1.5m/s and a constant sliding distance of 2100m. The variations in wear rate of spray formed Al-Graphite and Al-Si-Pb alloys with load are shown in Fig. 4.19. Wear rate increases with the increase in applied load for both alloys.

The variation in wear rate of spray formed Al–Si-Pb alloys on load showed that the wear rate is mild at low load and increased steeply at high load. It had been argued that repeated welding and fracture through weak metal causes the wear when sliding takes place between two surfaces. Under a low applied load, the friction causes some deformation and work hardening of its surface layer. Smearing and oxidation of Pb resulted as the wear debris is produced by cracking and spalling upon repeated stressing in ambient atmosphere. Once the oxidized layer of Pb is formed, the welding and work hardening of contact surface is greatly reduced due to the lubricating effect of the smeared lead oxide layer.

At higher load, on the other hand, welding and deformation are much more enhanced. Therefore, higher wear rate results due to strongly increased cracking and spalling. Furthermore, lubrication effect of Pb is greatly reduced because the Pb oxide layer smeared on the friction surface will be broken up at high load. This should also lead to the increase of wear rate.

It is observed that wear rate for Aluminum-Graphite is more as compared with that of Al-Si-Pb because of lower hardness of Aluminum-Graphite alloy.

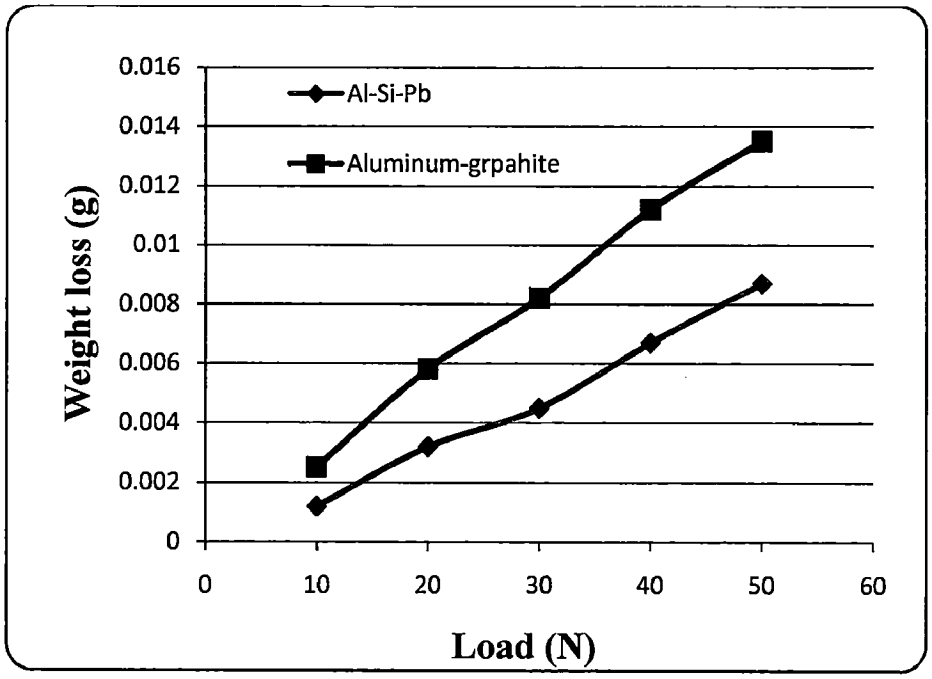


**Figure 4.19** Variation in wear rate of Al-Graphite and Al-Si-Pb alloys as a function of applied load.

The variations in coefficient of friction with load for spray formed Al-Graphite and Al-Si-Pb alloys are shown in Fig. 4.20. Coefficient of friction decreases with increasing load for both the alloys. The coefficient of friction decreased rapidly upto the load of 30N and beyond this load the friction coefficient was almost constant.

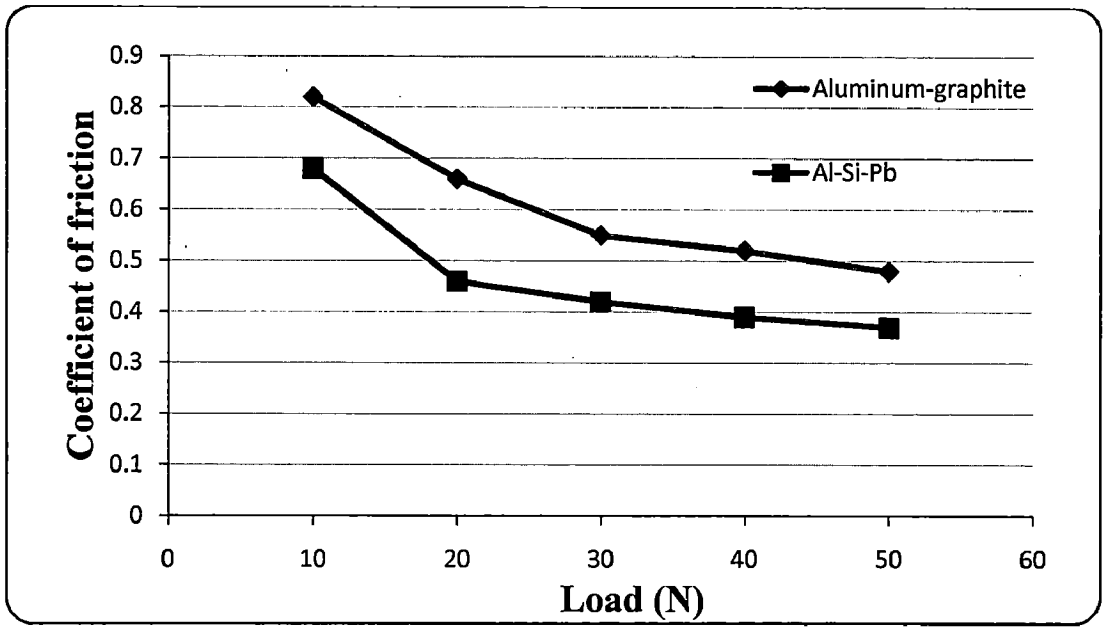


**Figure 4.20** Variation in coefficient of friction of Al-Graphite and Al-Si-Pb with applied load.

## 4.5 ANN (ARTIFICIAL NEURAL NETWORK) STRUCTURE

The ANN was constructed with one input array containing the values of different percentage reduction in thickness of aluminum graphite alloy, one hidden layers, and one output array. The determination of the number of neurons in the hidden layer is more art than science. A very rough rule of thumb is given by NeuralWare (Commercial software used for constructing and training ANN's) as:

$$h = \frac{number\ of\ training\ cases}{5(m+n)}$$

Where, h is the number of neurons in the hidden layer,

m, is the number of neurons in the output layer, and

n, is the number of neurons in the input layer.

In this study, a trial-and-error method is performed to optimize the number of neurons in the hidden layers. It was found that the network with one hidden layers and two neurons in that hidden layer fits well in the proposed ANN. Architecture of the ANN is shown in Figure 4.21.

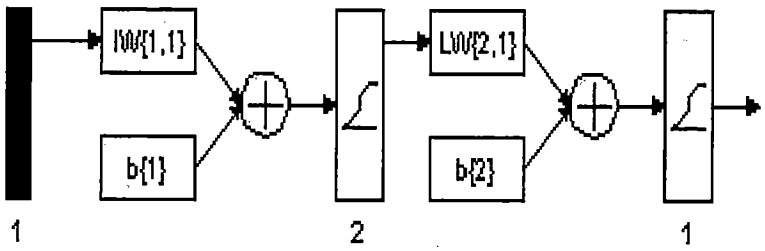


**Figure 4.21** ANN Architecture

A data set consists of 17 experimental data points were used to construct fully developed feed forward back propagation network. For the training problem at hand the following parameters were found to give good performance and rapid convergence of neural network: sigmoid logistic is the activation functions in both hidden and output layers. Testing of the trained network was set to one testing cycle per 100 training cycles. Testing is used to examine if the network is good enough to do the prediction, if not testing still runs the training process to reach threshold error.

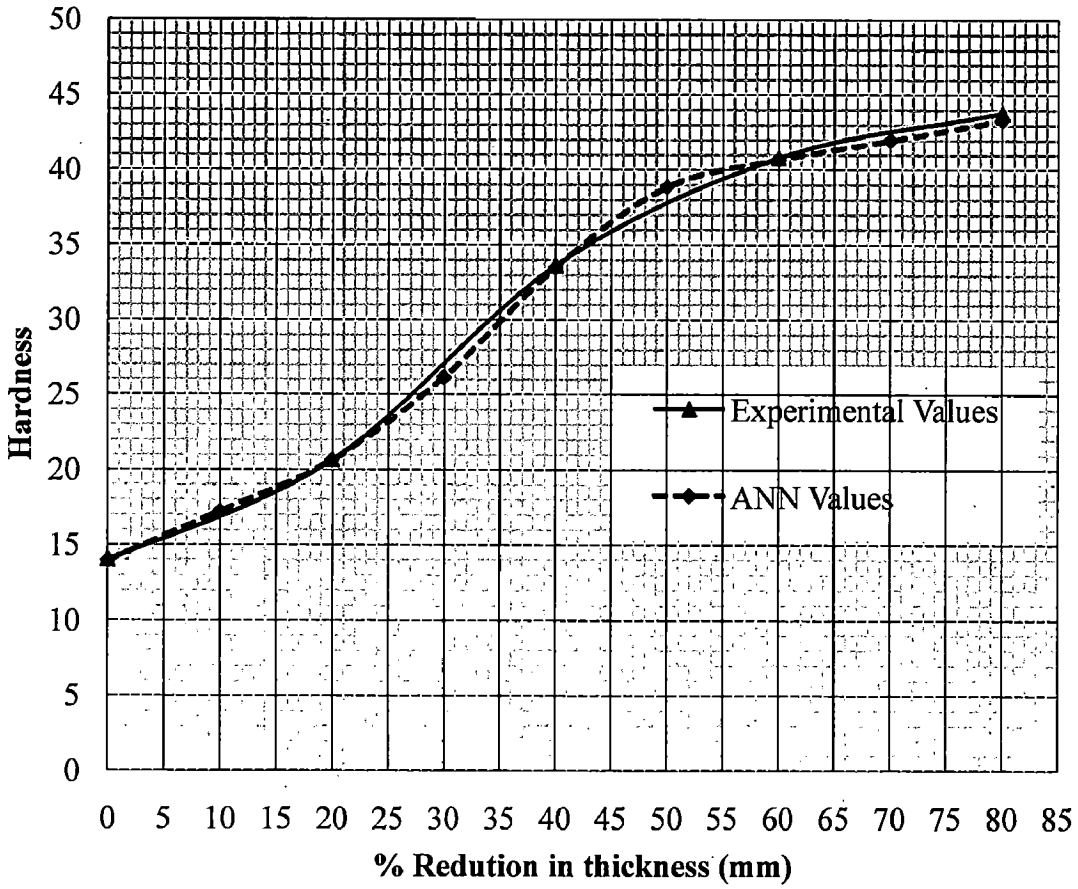


**Figure 4.22** Experimental results versus ANN results in hardness test for aluminum-graphite alloy.

To test the generalization performance of the trained network in training and testing processes, the experimental values were compared to the predicted values resulted from ANN as shown in Figure 4.22. After training and testing processes were finished, the ANN can be recalled to do prediction effectively. Figure 4.22 show the comparison between experimental and ANN results for some alloys tested in this study. Continuous lines represent experimental values and dashed lines represent ANN output. As seen from these figures, satisfactory agreement between the experimental and ANN results were obtained from using this type of neural network.

# Chapter 5

# CONCLUSIONS

The following conclusions are drawn from the above study:

1) From optical microstructures it has been concluded that spray forming is an appropriate route to produce immiscible metal alloy composites with uniform distribution of second phase particles.
2) Size and distribution of the matrix and second phase particles are depends on processing parameters (travelling distance, turbulence, rotation speed of the substrate).
3) Equi-axed grain structure of aluminum with lead and silicon at the grain boundaries has been observed.
4) The hardness of Al-Si-Pb is more compared with Al-Graphite due to ultra-fine and homogeneous lead phase distributed in the aluminum matrix and lead crystallite grain size still is in the nanometer range after spray forming, and also that there is amorphous areas distribution in the aluminum matrix.
5) The wear of Al-Graphite and Al-Si-Pb alloys increases linearly with increasing in applied load.
6) Predicted ANN values are similar to the Experimental values.

# Chapter 6

# SCOPE FOR FURTHER WORK

The following suggestions are felt necessary for further work related to characterization of spray formed aluminum alloys

1. Porosity, ultimate tensile strength, thermal conductivity, coefficient of thermal expansion can also be calculated for spray formed aluminum alloys.
2. The modeling of shape and porosity of perform can be done for spray forming.
3. Modeling using neural network can also be carried out for wear results.

# REFERENCES


[1] M.Gupta, S.C.Lim, .B.Ng, Mater, Sci. Technol. 13, (1997) 584–589.

[2] Sharma A. and Rajan T.V., "Bearing characteristics of cast leaded Aluminum-Silicon alloys", Wear. 197, (1996) 105–114.

[3] Pathak J.P., Torabian H. and Tiwari S.N., "Antiseizure and antifriction characteristics of Al-Si-Pb alloys", Wear. 202, (1997) 134-141.

[4] F. Akhlaghi, S.A. Pelaseyyed, "Characterization of aluminum/graphite particulate composites synthesized using a novel method termed in-situ powder metallurgy" Materials Science and Engineering A 385, (2004) 256.

[5] J., Liu Y.B., Lu Y., "The influence of Pb on the friction and wear behavior of Al-Si-Pb alloys", Materials Science and Engineering A 373, (2004) 294–302.

[6] J., Dong C. and Zhang Q.Y., "Improvement of the wear behavior of stir cast Al-Si-Pb alloys by hot extrusion", Tribol. Int., 36, (2003) 25–34.

[7] Mohan S., Agarwala V. and Ray S., "The effect of lead content on the wear characteristics of a stir-cast Al-Pb alloy", Wear, 140, (1990) 83–92.

[8] Fang X., Fan Z., "Rheo – diecasting of Al-Si-Pb immiscible alloys", Scripta mater., 54, (2006) 789–793.

[9] Suh Y.C. and Lee Z. H., "Nucleation of liquid Pb-Phase in hypermonotectic Al-Pb melt and the segregation of Pb droplets in melt – spun ribbon", Scripta metal. Mater., 33, (1995) 1231–1237.

[10] Zhao J.Z., Drees S. and Ratke L., "Strip casting of Al-Pb alloys – a numerical analysis", Material Science and Engineering, A 282, (2000) 262–269.

[11] Rudrakshi G.B., Srivastava V.C., Pathak J.P. and Ojha S.N., "Spray forming of Al-Si-Pb alloys and their wear characteristics", Material Science and Engineering, A 383, (2004) 30–38.

[12] Rudrakshi G.B., Srivastava V.C. and Ojha S.N., "Microstructural development in spray formed Al-3.5Cu-10Si-20Pb alloy and its comparative wear behavior in different environmental conditions", Material Science and Engineering, A 161, (2007) 100–108.

[13] P. S. Grant, "Spray Forming" Progress in Material Science 39, (1995) 397.

[14] Anand S., Srivastsan S., Wu Yue and Lavernia E.J., "Processing, microstructure and fracture behavior of a spray atomized and deposited Al-Si alloy", Material Science., 32, (1997) 2835–2848.

[15] Liang X., Earthman J.C. and Lavernia E.J., "On the mechanism of grain formation during spray atomization and deposition", Acta metal. Mater., 40, (1992) 3003–3016.

[16] Cai W. and Lavernia E.J., "Modeling of porosity during spray forming", Material Science and Engineering, A 226, (1997) 8–12.

[17] S.N.Tiwari and J.P Pathak, "Lead a potential soft phase alloying addition to Aluminum Bearing Alloys", Aluminum, vol.1-6, (1987) 41 –415.

[18] P.Rohtagi, "Metal matrix composites", Defence science journal, Vol. 43, (1993) 323–349.

[19] S.Mohan, "Fabrication of cast Al-Based Lead Bearing Alloys and their wear characteristic", Ph.D. Thesis, Met. Engg. Deptt., U.O.R., Roorkee (1989).

[20] Sharma A. and Rajan T.V., "Bearing characteristics of cast leaded Aluminum-Silicon alloys", Wear, 197, (1996) 105–114.

[21] Yu F., Dwarakadasa D.S. and Ranganathan S., "Microstructure and mechanical of spray fromed Al-Si-Pb alloys", J.Mater. Process. Techmo., 137, (2003) 164–167.

[22] Torabian H., Pathak J.P. and Tiwari S.N., "On wear characteristics of leaded Aluminum-Silicon alloys", Wear, 177, (1994) 47–54.

[23] M. Saravanan, R.M. Pillai, K.R. Ravi, B.C. Pai, M. Brahmakumar, "Development of ultrafine grain aluminum–graphite metal matrix composite by equal channel angular pressing", Composites Science and Technology 67, (2007) 1275.

[24] I. Estrada-Guela, C. Carreno-Gallardoa, D.C. Mendoza-Ruiza, M. Miki-Yoshidaa, E. Rocha-Rangel, R. Martínez-Sáncheza, "Graphite nanoparticle dispersion in 7075 aluminum alloy by means of mechanical alloying", Journal of Alloys and Compounds 483, (2009) 173.

[25] H.J. Li, L.H. Qi, H.M. Han, L.J. Guo, "Neural network modeling and optimization of semi-solid extrusion for aluminum matrix composites", Journal of Materials Processing Technology 151, (2004) 126–132.

[26] Mohammed Hayajneh, Adel Mahamood Hassan, Abdalla Alrashdan, Ahmad Turki Mayyas, "Prediction of tribological behavior of aluminum–copper based composite using artificial neural network", Journal of Alloys and Compounds 470, (2009) 584–588.

7] Adel Mahamood Hassan, Abdalla Alrashdan, Mohammed T. Hayajneh, Ahmad Turki Mayyas, "Prediction of density, porosity and hardness in aluminum–copper-based composite materials using artificial neural network", Journal of materials processing technology 209, (2009) 894–899.

28] Prashant Khare, Varun Garg, Devendra Singh, "Formation of aluminum-graphite composite by spray forming technique", (2008).